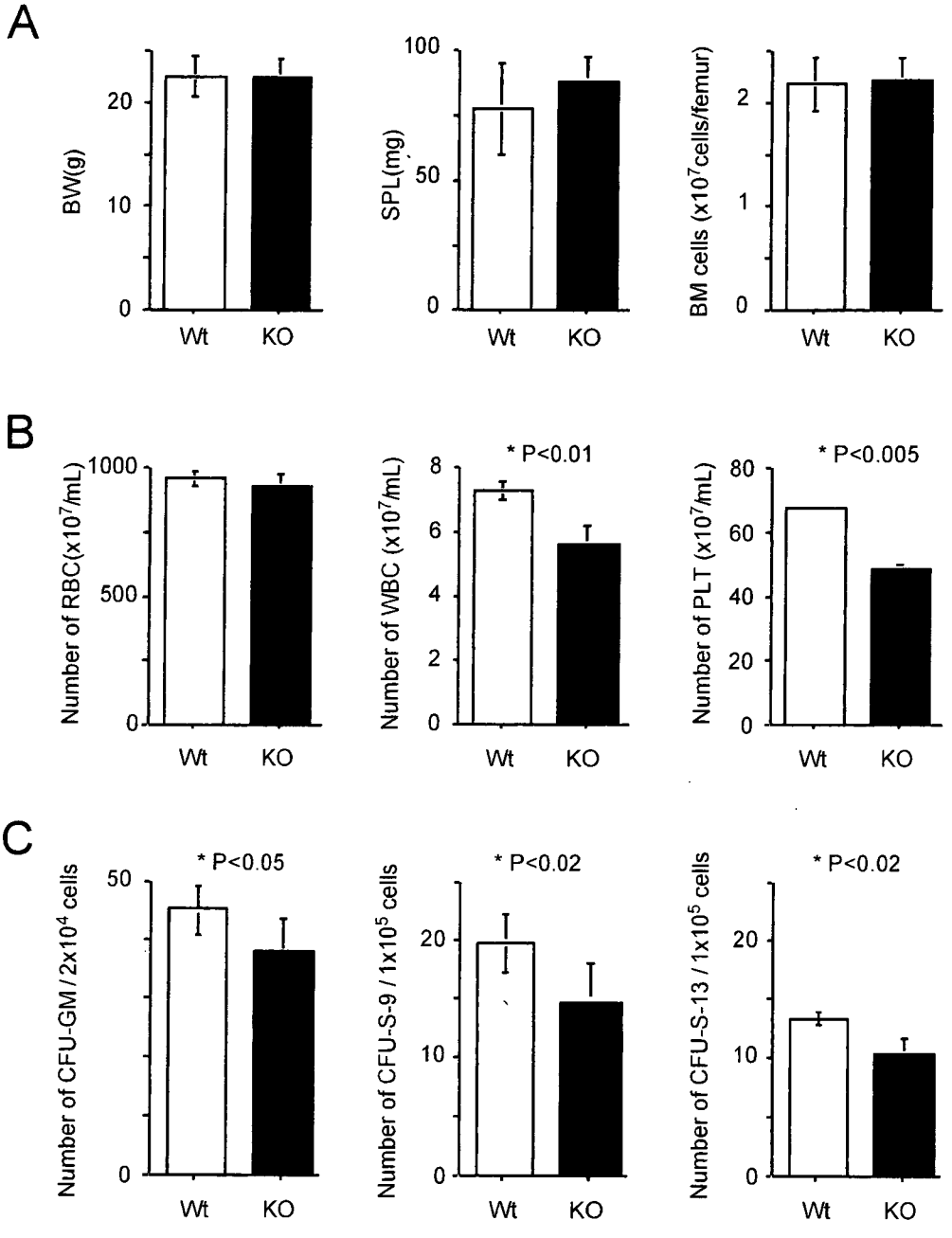

Figure 4. Parameters associated with steady-state hematopoiesis. Row A: from left, body weight (BW), splenic weight (SPL), and bone marrow cellularity (BM cells; $n = 6$ in each genotype). Row B: from left, numbers of peripheral blood cells—red blood cells (RBCs), white blood cells (WBCs), and platelets (PLTs; $n = 6$ for each genotype). Row C: from left; numbers of hematopoietic progenitor cells in steady-state CFU-GMs, hematopoietic progenitor cells for CFU-S-9s, and those for CFU-S-13s. Three donor mice were used for each genotype, and six mice were used for each recipient group. Open box, wild type; solid box, Cx32-KO; vertical bar, standard deviation of the mean. *Difference between wild-type and Cx32-KO mice is significant (P values are indicated in each figure).

shaded column from the left), Cx32-KO mice produced significantly smaller colonies due to as yet undetermined reasons.

Regeneration Potency of Bone Marrow Cells from Cx32-KO Mice and Wild-Type Mice. Treatment with 5-fluorouracil (5-FU) induces a temporary arrest of hematopoietic progenitor cell proliferation, except in the very immature hematopoietic progenitor cell compartment (30–32), in which mature hematopoietic progenitor cells are killed, whereas immature dormant HSCs selectively survive. The number of CFU-GMs per unit number of bone marrow cells was counted for 2 weeks after the 5-FU treatment. As shown in Figure 6, the number of CFU-GMs in both wild-type mice and Cx32-KO mice increased rapidly after 5-FU treatment; however, the increase in the number of CFU-GMs seemed to be delayed in Cx32-KO mice compared with that of wild-type mice.

Experimental Leukemogenesis: Whole-Body

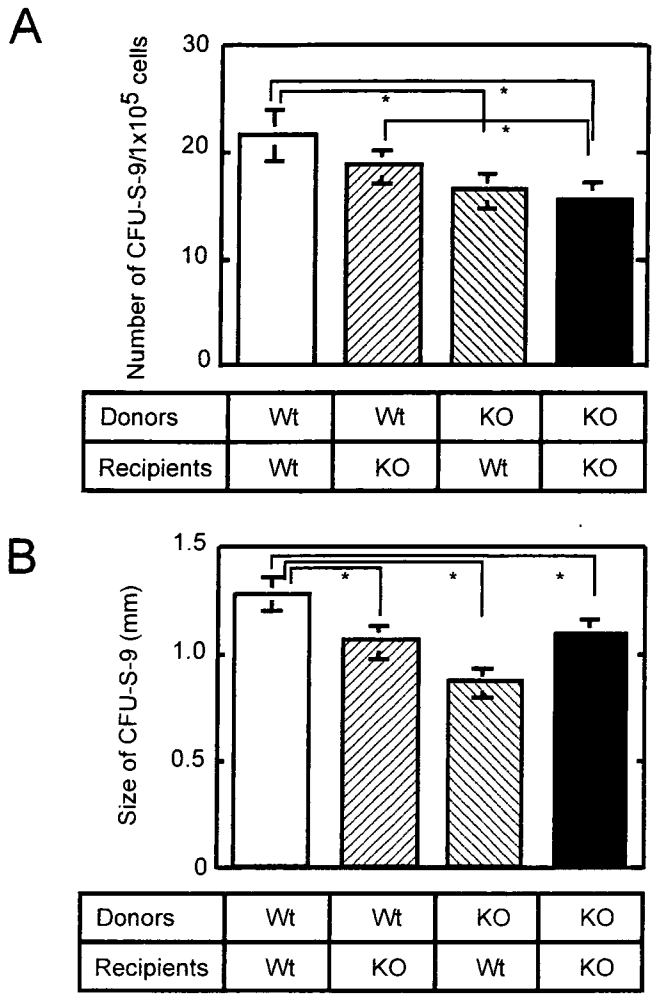

Figure 5. Number and size of CFU-Ss assayed in four different combinations between donors, either wild-type or Cx32-KO bone marrow cells, and lethally irradiated recipients, either wild-type or Cx32-KO mice. (A) Number of CFU-S-9s. (B) Size of CFU-S-9s. *Differences between each bar connected with a line are significant ($P < 0.05$); three donor mice were used for each genotype, and six mice were used for each recipient group.

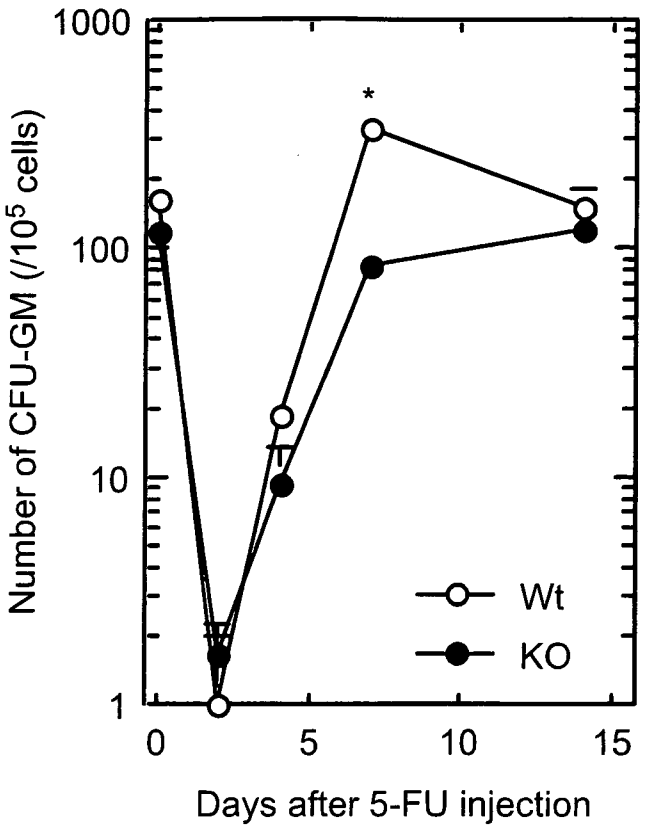

Figure 6. Changes in number of CFU-GMs in femoral bone marrow cells in wild-type or Cx32-KO mice (days after a single dose of 5-FU, iv, 150 mg/kg body wt). Open circle, wild type; closed circle, Cx32-KO. *Seven days after 5-FU injection, at which time the difference between the wild-type and Cx32-KO mice was significant ($P < 0.05$); three mice each were used for each data point).

Bioassay and the Transplantation Bioassay With or Without Cx32. *Cx32-KO Hematopoietic Progenitor Cells and Leukemogenesis.* A high incidence of hematopoietic neoplasms was observed during the MNU-induced leukemogenesis in Cx32-KO mice. The survival curves of the mice of each group showed that the MNU-treated mice, regardless of genotype, died much earlier because of MNU-induced hematopoietic malignancies and other diseases (Fig. 7A). Untreated control mice, regardless of genotype, gradually started to die 400 days after the treated groups received an MNU.

The percentage of incidences of hematopoietic malignancies in mice treated with MNU, both wild-type and Cx32-KO, and mice in both nontreated control groups are shown in Figure 7B. When Cx32 was knocked out, the incidence of hematopoietic malignancies started to increase rapidly 100 days after MNU treatment (closed squares), which exceeded the incidence of hematopoietic malignancies in wild-type mice (50.0%), and reached 91.7% ($P < 0.05$ by Fischer exact test). The incidence of hematopoietic neoplasms in nontreated groups of both wild-type and Cx32-KO mice as reference groups increased gradually, reaching 40.0% for the wild-type mice and 33.3% for Cx32-KO mice. Concomitantly, hepatomas developed in both groups of mice after 664 days of age, and the incidence in Cx32-KO mice was higher than that in wild-type mice, although it was statistically less significant (33.3% and 10.0%, respectively; data not shown).

Assay of Leukemogenicity: The Transplantation Assay in Cx32-KO Bone Marrow Cells and Wild-Type Bone Marrow Cells. Because the incidence of hematopoietic malignancies was significantly high in Cx32-KO mice (Fig. 7B), but the development of hematopoietic malignancies was interfered with by malignancies from other tissues and organs due to competitive risk of the tumorigenicity (data not shown and Ref. 22), lethally irradiated same wild-type mice were repopulated with either bone marrow cells from wild-type mice or Cx32-KO mice, and the development of hematopoietic neoplasms after a single dose of MNU was observed under the same recipient

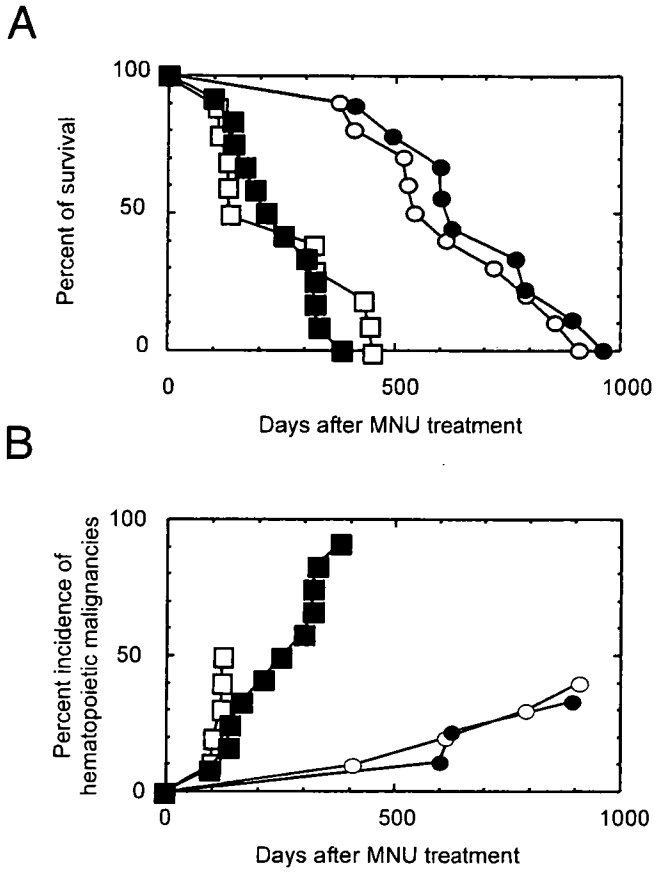

Figure 7. Whole-body assay of hematopoietic malignancies by a single dose of MNU at 50 mg/kg body wt. (A) Survival fraction. (B) Cumulative incidences of hematopoietic malignancies in Cx32-KO mice or wild-type mice with or without a single ip injection of MNU. Open circle, wild type without MNU injection, 10 mice; open square, wild type with MNU injection, 10 mice; closed circle, Cx32-KO without MNU injection, 9 mice; closed square, Cx32-KO with MNU injection, 12 mice.

conditions (the transplantation assay). However, few differences in survival time and incidence of neoplasms were observed between mice repopulated with wild-type bone marrow cells and those repopulated with Cx32-KO bone marrow cells (data not shown).

Competitive Assay of Leukemogenicity Between Cx32-KO Bone Marrow Cells and Wild-Type Bone Marrow Cells. A mixed population of bone marrow cells from Cx32-KO and wild-type mice was injected into lethally irradiated wild-type mice, and the incidence of hematopoietic malignancies competitively caused by bone marrow cells from Cx32-KO mice and those from wild-type mice was determined under the same *in vivo* conditions of the recipient (the competitive assay). Figure 8 shows the incidences of hematopoietic malignancies in mice that received a single dose of MNU at either 75 mg/kg body wt (dark squares) or 50 mg/kg body wt (medium squares), compared with the nontreated control (light squares), which are plotted against the days after MNU treatment. The incidence of hematopoietic malignancies of the 75 mg/kg body wt MNU-treated group reached 88.9%, whereas that of

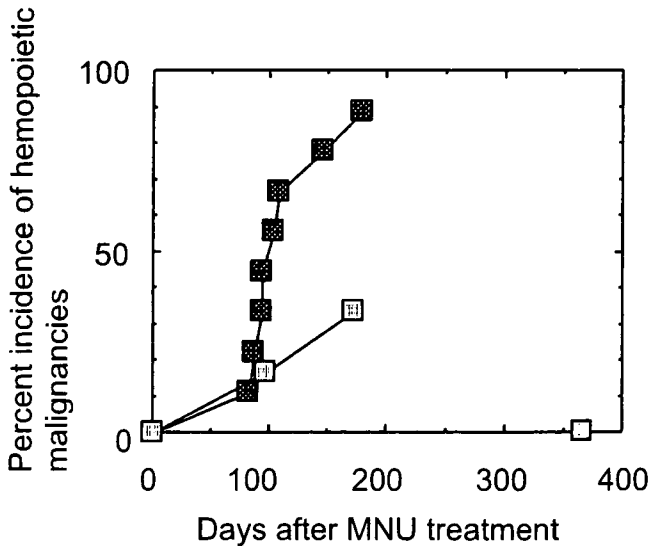

Figure 8. Competitive bone marrow transplantation bioassays repopulated with mixture of bone marrow cells from wild-type and Cx32-KO mice, followed by a single dose of MNU. Cumulative incidences of hematopoietic malignancies in the group repopulated with the mixture cells followed by a single ip injection of MNU at 50 or 75 mg/kg body wt. Light square, vehicle treatment; medium squares, 50 mg treatment; dark squares, 75 mg treatment.

the 50 mg/kg body wt MNU-treated group reached 33.3%. The incidences of hematopoietic neoplasms that were observed in the competitive assays are shown in Table 1. In the mice treated with MNU at 50 mg/kg body wt and in those treated with 75 mg/kg body wt, two and eight hematopoietic neoplasms developed, respectively.

Samples from these neoplasms were analyzed for their genotype to determine whether the neoplasms originated from bone marrow cells of wild-type mice or Cx32-KO mice (Fig. 9). In Figure 9, lanes 1, 2, 4, 5, 6, 8, and 9 show the presence of the gene inserted for the knockout strategy; thus, the neoplastic samples in these lanes were identified as having originated from bone marrow cells of Cx32-KO mice. The origins of the hematopoietic neoplasms are shown in Table 1. The results show that the malignancies originated from the bone marrow cells of Cx32-KO mice in two of two leukemias in the 50 mg/kg body wt MNU-treated group, and in seven of eight leukemias in the 75 mg/kg body wt MNU-treated group.

Discussion

The role of Cx32 in steady-state hematopoiesis and its potential protective role of prevention during leukemogenesis were analyzed in this study. In this study we demonstrated for the first time that a Cx gene, namely, the Cx32 gene, is expressed in hematopoietic stem/progenitor cells, and in the case of Cx32-KO mice, the regeneration of bone marrow after chemical abrasion was clearly delayed, which suggests a beneficial role of Cx32 in the regeneration. Furthermore, the incidence of MNU-induced leukemia was

Table 1. Transplantation Bioassays for Repopulation with Mixture of Bone Marrow Cells Followed by Induction of Tumor by MNU, and Genotyping of Tumor Origin

		Tumor origin, no. (%)	
Dose of MNU	No. of tumors	Wild type	KO
50 mg/kg body wt	2	0 (0)	2 (100)
75 mg/kg body wt	8	1 (12.5)	7 (87.5)

clearly high in Cx32-KO mice after a single administration of MNU, as shown not only in the whole-body assay (Fig. 7) but also in the competitive repopulation assay using bone marrow cells from Cx32-KO and wild-type mice (Figs. 8 and 9). These results are compatible with the observation of epithelial tumorigenesis in the liver and lungs observed in the same Cx32-KO strain (9), and this is the first observation in leukemogenesis.

Various Cxs are expressed in stromal cells of the fetal liver (Cxs 43, 45, 30.3, 31, and 31.1) and bone marrow (Cxs 43, 45, and 31; Ref. 13). However, the contribution of Cxs to hematopoiesis was found only on the basis of the effect of Cxs *via* stromal cell dependence; consequently, no Cxs were previously found in hematopoietic stem cells and/or progenitor cells (16). For us this is interesting, because hematopoietic progenitor cells possess morphologic evidence as well as functional evidence for cellular communication with each other (33, 34). Interestingly, in our recent study, Cx32-KO mice exposed to benzene showed a hematopoietic impairment; however, the site of this impairment was not identified in either hematopoietic progenitor or stromal cells (15).

Thus, we first determined whether hematopoietic progenitor cells express Cx32 molecules; however, as reported elsewhere, Cx32 is not detected in the bone marrow (Fig. 1A and Refs. 15 and 19). Interestingly, hematopoietic spleen colonies derived from hematopoietic progenitor cells were found to express Cx32 (Fig. 1B). This observation was further supported by the immunohistochemical reaction of cells in the colonies to the anti-Cx32 antibody, in which Cx32-positive cells were only scattered along the border of each colony (Figs. 2Aa and b). Furthermore, flow cytometry using the anti-Cx32 antibody after performance of the combination of immunobead-density gradient separation and the immunomagnetic bead separation showed that the Cx32-positive fraction was found to belong to the HSC compartment and was calculated as only 0.27% with respect to the unseparated bone marrow cells (Fig. 3). These findings may be in good agreement with a previous report of the absence of Cx32 expression in the bone marrow tissue (13). A hematopoietic disadvantage in progenitor cells associated with Cx32 deficiency was further evident, because all progenitor cells from the bone marrow of Cx32-KO mice showed a ~20% decrease in numbers of CFU-S-13s, CFU-S-9s, and CFU-GMs. Thus, it can be concluded that Cx32 is required for maintaining normal hematopoiesis, specifically during the maturation of hematopoietic stem cells to the progenitor cells.

However, whether Cx32 also is functional in differentiated mature blood cells is questionable, despite the observation that the numbers of white blood cells and platelets were significantly lower in the peripheral blood of the Cx32-KO mice than in the wild-type mice (Fig. 4B). It is of interest to calculate a probability of Cx32-positive cells based on this ratio of those Cx32-positive bone marrow cells out of the $lin^+c\text{-}kit^-$ fraction; that is, only 0.0093% with respect to that of unfractionated original bone marrow cells (data not shown). Because our repeated analyses failed to detect Cx32 expression in mature blood cells, the decreased numbers of white blood cells and platelets in the Cx32-KO mice are regarded as a reflection of the shortage of immature progenitor cell compartments due to the lack of Cx32 at the level of stem cells and progenitor cells.

The bone marrow transplantation in different combinations of the donor and recipient, which was repopulated with bone marrow cells from either wild-type mice or Cx32-KO mice, showed a small number of spleen colonies in the groups repopulated with Cx32-KO bone marrow cells. Interestingly, as shown in Figure 5B, colonies derived from the same Cx32-KO bone marrow cells showed significantly smaller colonies regardless of the genotype of recipients—that is, wild-type or Cx32-KO mice—presumably owing to

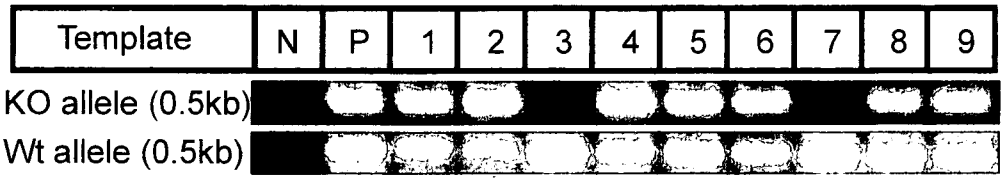

Figure 9. Genotyping of hematopoietic neoplasms whose origin was identified by genomic PCR. N, negative control for PCR without DNA; P, positive control for PCR using genomic DNA from the $Cx32^{+/-}$ hepatic tissue. Lanes 1–9, DNA extracted from hematopoietic neoplasms that developed during assay of bone marrow transplantation. Lane 3, control neoplasm that developed in mouse repopulated with wild-type bone marrow cells. Lane 4, control neoplasm that developed in mouse repopulated with Cx32-KO bone marrow cells. Lanes 1, 2, and 5–9, neoplasms that developed in mice repopulated with a mixture of bone marrow cells from wild-type and Cx32-KO mice. Note that lane 7 has a faint band for the KO allele, which shows an additional simultaneous expression band from the repopulated normal hematopoietic cells. For lanes 1, 2, 5, 6, 8, and 9, the tumors arising from Cx32-KO bone marrow cells show double bands, namely a Wt allele and another allele for KO strategy. Intensities of these bands are identical compared with that of lane 4.

the lack of Cx32 expression in the hematopoietic progenitor cells (shaded column second from the right vs. closed column far right). The reason why a small size of colonies observed in the Cx32-KO recipient mice received wild-type bone marrow cells cannot be answered in the present study. It is possible that Cx32 deficiency in combination with a lethal dose of whole-body irradiation for the bone marrow transplantation induces an unknown synergistic damage. Our previous observation that Cx32-KO mice treated repeatedly with a dose of benzene by inhalation showed a severe chemical-induced persistent pulmonary injury (15) may be relevant to the present observation. Stem cell regeneration after chemical abrasion with 5-FU was delayed in Cx32-KO mice (Fig. 6), which indicates that early recovery of mice also requires the growth of hematopoietic progenitor cells expressing Cx32. This is compatible with the observation of transgenic mice expressing a dominant-negative mutant of Cx32, which showed a notably delayed recovery after partial hepatectomy (5).

The role of Cx32 is associated with the prevention of carcinogenicity, as an initiation of leukemogenicity was preferentially induced in Cx32-KO mice by a single dose of MNU; thus, Cxs likely have a protective function against leukemogenicity, specifically for the initiation of the carcinogenic process. Phenotypically, the results are compatible with the observation that spontaneous hepatic tumors and diethyl-nitrosamine–induced hepatic tumors tended to develop in Cx32-KO mice compared with wild-type mice (9). Furthermore, radiation-induced hepatocarcinogenesis and diethyl-nitrosamine–induced pulmonary tumorigenesis showed a high frequency of tumorigenesis in Cx32-KO mice (35, 36), which also is compatible with the results of the present study.

Why does the lack of Cxs result in more frequent carcinogenesis? Why was the incidence of leukemogenesis higher in Cx32-KO mice (Fig. 7B, closed squares)? Furthermore, why did leukemogenicity in the wild-type mice appear earlier than that in Cx32-KO mice, although the total incidence remains lower by about 50% (Fig. 7B, open squares) than in the Cx32-KO mice (Fig. 7B, open squares vs. closed squares, respectively). The present study implies that Cx32-KO mice showed a high frequency of leukemogenesis due in part, to a possible suppression of apoptosis of hematopoietic progenitor cells after exposure to chemical carcinogens, and thereby the initiation of leukemogenicity was induced frequently in Cx32-KO mice. Cx32 is, therefore, surmised to protect hematopoietic progenitor cells from leukemogenic triggers in the wild-type mice.

The present competitive assay clearly showed that Cx32-KO bone marrow cells have a higher risk of becoming leukemogenic. The above-mentioned findings in this study imply that Cxs play an essential role in tumor suppression, although a temporary disconnection of Cxs induced by so-called carcinogenic promoter chemicals might induce an independent growth of possible neoplastic candidates, which may, however, eventually undergo apoptosis or be enclosed by cells with recovered Cx function.

Lastly, our results indicate that the risk of developing leukemia in patients with X chromosome–linked Cx32 deficiency, called Charcot-Marie-Tooth syndrome, might not be incidental.

This study is dedicated to the late Dr. Eugene P. Cronkite for his fifth-year memorial. We thank Dr. Y. Kawasaki, Dr. K. Sai, Ms. E. Tachihara, Ms. N. Moriyama, Ms. Y. Shinzawa, Ms. Y. Usami, Mr. K. Terasaka, and Mr. Morita for excellent technical assistance, and Ms. N. Kikuchi, Ms. M. Yoshizawa, and Ms. M. Hojo for secretarial assistance.

1. Loewenstein WR. Junctional intercellular communication and the control of growth. Biochim Biophys Acta 560:1–65, 1979.
2. Wilson MR, Close TW, Trosko JE. Cell population dynamics (apoptosis, mitosis, and cell-cell communication) during disruption of homeostasis. Exp Cell Res 254:257–268, 2000.
3. Bruzzone R, White TW, Paul DL. Connections with connexins: the molecular basis of direct intercellular signaling. Eur J Biochem 238:1–27, 1996.
4. Trosko JE, Chang CC, Madhukar BV. Modulation of intercellular communication during radiation and chemical carcinogenesis. Radiat Res 123:241–251, 1990.
5. Dagli ML, Yamasaki H, Krutovskikh V, Omori Y. Delayed liver regeneration and increased susceptibility to chemical hepatocarcinogenesis in transgenic mice expressing a dominant-negative mutant of connexin32 only in the liver. Carcinogenesis 25:483–492, 2004.
6. Mesnil M. Connexins and cancer. Biol Cell 94:493–500, 2002.
7. King TJ, Gurley KE, Prunty J, Shin JL, Kemp CJ, Lampe PD. Deficiency in the gap junction protein connexin32 alters p27Kip1 tumor suppression and MAPK activation in a tissue-specific manner. Oncogene 24:1718–1726, 2005.
8. Trosko JE, Ruch RJ. Cell-cell communication in carcinogenesis. Front Biosci 3:D208–D236, 1998.
9. Temme A, Buchmann A, Gabriel HD, Nelles E, Schwarz M, Willecke K. High incidence of spontaneous and chemically induced liver tumors in mice deficient for connexin32. Curr Biol 7:713–716, 1997.
10. Jeong SH, Habeebu SS, Klaassen CD. Cadmium decreases gap junctional intercellular communication in mouse liver. Toxicol Sci 57:156–166, 2000.
11. Rosendaal M, Gregan A, Green CR. Direct cell-cell communication in the blood-forming system. Tissue Cell 23:457–470, 1991.
12. Ploemacher RE, Mayen AE, De Koning AE, Krenacs T, Rosendaal M. Hematopoiesis: gap junction intercellular communication is likely to be involved in regulation of stroma-dependent proliferation of hemopoietic stem cells. Hematology 5:133–147, 2000.
13. Cancelas JA, Koevoet WL, de Koning AE, Mayen AE, Rombouts EJ, Ploemacher RE. Connexin-43 gap junctions are involved in multiconnexin-expressing stromal support of hemopoietic progenitors and stem cells. Blood 96:498–505, 2000.
14. Montecino-Rodriguez E, Leathers H, Dorshkind K. Expression of connexin 43 (Cx43) is critical for normal hematopoiesis. Blood 96: 917–924, 2000.
15. Yoon BI, Hirabayashi Y, Kawasaki Y, Tsuboi I, Ott T, Kodama Y, Kanno J, Kim DY, Willecke K, Inoue T. Exacerbation of benzene pneumotoxicity in connexin 32 knockout mice: enhanced proliferation of CYP2E1-immunoreactive alveolar epithelial cells. Toxicology 195: 19–29, 2004.
16. Krenacs T, Rosendaal M. Connexin43 gap junctions in normal, regenerating, and cultured mouse bone marrow and in human

leukemias: their possible involvement in blood formation. Am J Pathol 152:993–1004, 1998.

17. Keller JR, Mantel C, Sing GK, Ellingsworth LR, Ruscetti SK, Ruscetti FW. Transforming growth factor beta 1 selectively regulates early murine hematopoietic progenitors and inhibits the growth of IL-3-dependent myeloid leukemia cell lines. J Exp Med 168:737–750, 1988.
18. Sasaki H, Matsuda M, Lu Y, Ikuta K, Matsuyama S, Hirabayashi Y, Mitsui H, Matsumura T, Muramatsu M, Tsukada T, Aizawa S, Inoue T. A fraction unresponsive to growth inhibition by TGF-beta among the high-proliferative potential progenitor cells in bone marrow of p53-deficient mice. Leukemia 11:239–244, 1997.
19. Nelles E, Butzler C, Jung D, Temme A, Gabriel HD, Dahl U, Traub O, Stumpel F, Jungermann K, Zielasek J, Toyka KV, Dermietzel R, Willecke K. Defective propagation of signals generated by sympathetic nerve stimulation in the liver of connexin32-deficient mice. Proc Natl Acad Sci U S A 93:9565–9570, 1996.
20. Yoon BI, Hirabayashi Y, Kawasaki Y, Kodama Y, Kaneko T, Kim DY, Inoue T. Mechanism of action of benzene toxicity: cell cycle suppression in hemopoietic progenitor cells (CFU-GM). Exp Hematol 29:278–285, 2001.
21. Sander B, Andersson J, Andersson U. Assessment of cytokines by immunofluorescence and the paraformaldehyde-saponin procedure. Immunol Rev 119:65–93, 1991.
22. Hirabayashi Y, Inoue T, Suda Y, Aizawa S, Ikawa Y, Kanisawa M. Hemopoietic neoplasms in lethally irradiated mice repopulated with bone marrow cells carrying the human c-myc oncogene: a repopulation assay. Exp Hematol 20:167–172, 1992.
23. Till JE, McCulloch EA. A direct measurement of the radiation sensitivity of normal mouse bone marrow cells. Radiat Res 14:213–222, 1961.
24. Hirabayashi Y, Matsuda M, Aizawa S, Kodama Y, Kanno J, Inoue T. Serial transplantation of p53-deficient hemopoietic progenitor cells to assess their infinite growth potential. Exp Biol Med (Maywood) 227: 474–479, 2002.
25. Inoue T, Cronkite EP, Commerford SL, Carsten AL. Residual toxicity in hematopoietic cells following a single dose of methylnitrosourea. Leuk Res 8:105–116, 1984.
26. Hirabayashi Y, Yoshida K, Aizawa S, Kodama Y, Kanno J, Kurokawa Y, Yoshimura I, Inoue T. Evaluation of nonthreshold leukemogenic response to methyl nitrosourea in p53-deficient C3H/He mice. Toxicol Appl Pharmacol 190:251–261, 2003.
27. Hirabayashi Y, Inoue T, Yoshida K, Inayama Y, Kanisawa M. The detection of normal hidden stem cells during the development of leukemia: assays with PGK isozyme. Exp Hematol 18:7–10, 1990.
28. Tanaka T, Suda T, Suda J, Inoue T, Hirabayashi Y, Hirai H, Takaku F, Miura Y. Stimulatory effects of granulocyte colony-stimulating factor on colony-forming units-spleen (CFU-S) differentiation and pre-CFU-S proliferation in mice. Blood 77:2597–2602, 1991.
29. Magli MC, Iscove NN, Odartchenko N. Transient nature of early haematopoietic spleen colonies. Nature 295:527–529, 1982.
30. Shibagaki T, Inoue T, Kubota N, Kanisawa M. Fraction of pluripotent hemopoietic stem cells in DNA synthesis varies with generation age. Exp Hematol 14:794–797, 1986.
31. Rosendaal M, Hodgson GS, Bradley TR. Organization of haemopoietic stem cells: the generation-age hypothesis. Cell Tissue Kinet 12:17–29, 1979.
32. Ogawa M, Bergsagel DE, McCulloch EA. Sensitivity of human and murine hemopoietic precursor cells to chemotherapeutic agents assessed in cell culture. Blood 42:851–856, 1973.
33. Campbell FR. Gap junctions between cells of bone marrow: an ultrastructural study using tannic acid. Anat Rec 196:101–107, 1980.
34. Campbell FR. Intercellular contacts between migrating blood cells and cells of the sinusoidal wall of bone marrow. An ultrastructural study using tannic acid. Anat Rec 203:365–374, 1982.
35. King TJ, Lampe PD. Mice deficient for the gap junction protein Connexin32 exhibit increased radiation-induced tumorigenesis associated with elevated mitogen-activated protein kinase (p44/Erk1, p42/Erk2) activation. Carcinogenesis 25:669–680, 2004.
36. King TJ, Lampe PD. The gap junction protein connexin32 is a mouse lung tumor suppressor. Cancer Res 64:7191–7196, 2004.

ELSEVIER

EXPERIMENTAL HEMATOLOGY

Experimental Hematology 35 (2007) 125–133

Implications of hemopoietic progenitor cell kinetics and experimental leukemogenesis: Relevance to Gompertzean mortality as possible hematotoxicological endpoint

Yoko Hirabayashi[a] and Tohru Inoue[b]

[a]*Cellular and Molecular Toxicology Division, Center for Biological Safety and Research, National Institute of Health Sciences, Tokyo, Japan;* [b]*Center for Biological Safety and Research, National Institute of Health Sciences, Tokyo, Japan*

Objective. **The aim of this study is to investigate a possible implication in cell kinetics of the hematopoietic progenitors to the experimental leukemogenesis to elucidate the relevance of various leukemic mode of action to Gompertzean survival curves, a new parameter based on the lifespan.**

Materials and Methods. **Mice, C3H/He, and C57BL/6 strain, male and female, with or without genetic modifications, e.g., p53-deficiency or thioredoxin overexpression were used in the present hemopoietic stem/progenitor research, radiation- or benzene-induced leukemogenesis followed by histopathological examination. A lethal dose of radiation for bone marrow transplantation, and a graded increased dose up to 5 Gy of x-rays for induction of hematopoietic malignancies were given. For caloric restriction studies, 77 kcal/week was maintained in accordance to different restriction-timing. For assays of hematopoietic colonization, colony-forming unit spleen and colony-forming unit granulocyte macrophage were evaluated. Hematopoietic progenitor cell-specific kinetics were studied by continuous labeling of bromodeoxyuridine for cycling cells, followed by ultraviolet (UV) exposure and hemopoietic colonization (bromodeoxyuridine UV [BUUV] method). Various experimental survival curves were applied to a mathematical analysis by Gompertz-Makeham law of mortality.**

Results. **Referring current authors' studies on leukemogenesis induced by ionizing radiation and benzene exposure, implications of hematopoietic progenitor cell kinetics to the experimental leukemogenesis were evaluated by means of a novel experimental tool, the BUUV method. Comparative studies to elucidate relevancies of these data, including two prevention studies, one on caloric restriction and the other on antioxidative thioredoxin overexpression, to those Gompertzean survival curves of experimental animals were analyzed.**

Conclusion. **The Gompertzean expression may elucidate an appropriate toxicological endpoint for evaluating the effect of radiation and/or benzene-exposure on the lifespan and its modification by various experimental preventive measures.** © **2007 International Society for Experimental Hematology. Published by Elsevier Inc.**

The principle of the mortality rate of human beings was recognized by Gompertz [1] more than 180 years ago, who described that mortality rate during a unit time interval increases exponentially with lifetime. It was found that the Gompertzean expression can be applied to major mammalian species, and that the slope of the Gompertzean curve becomes shallower along the evolutionary hierarchy of the animal kingdom from rodents to humans. Moreover, when one applies the Gompertzean expression to a particular species, e.g., mice, one could note that regardless of type of compound, whether carcinogenic compounds or other life-threatening chemical compounds, the slope is steeper, indicating a shortening of lifespan not only attributable to carcinogenic impact but also cardiovascular, nephrotoxic, and other nontumorigenic diseases.

Radiation and benzene are the ultimate human leukemogens, known for over eight decades, on which the late Eugene P. Cronkite focused his attention and which he used to compare mechanisms of toxicities induced by radiation and benzene exposure [2,3]. His most notable strategy in studying mechanisms underlying leukemogenesis induced by

Offprint requests to: Yoko Hirabayashi, M.D., Ph.D., Cellular and Molecular Toxicology Division, Center for Biological Safety and Research, National Institute of Health Sciences, 1-18-1 Kamiyohga, Setagayaku, Tokyo 158-8501, Japan; E-mail: yokohira@nihs.go.jp

0301-472X/07 $–see front matter.
doi: 10.1016/j.exphem.2007.01.020

both compounds was to focus on the relevancy of the number and quality of hemopoietic stem/progenitor cells and their significance in stem/progenitor cell kinetics in relation to leukemogenicity. Because an increase in radiation dose exponentially decreases the number of hemopoietic progenitor cells (Fig. 1A, line "a"), exposure to an ionizing radiation of >5 Gy will not yield a high frequency of leukemias, but will induce a significant decrease in the incidence of leukemias, possibly because of the decrease in the number of hemopoietic progenitor cells (although it remains unclear whether stem/progenitor cells are leukemic target cells). The minimum number of potentially mutated stem/progenitor cells for the development of one case of leukemia decreases with increase in radiation dose (Fig. 1A, line "b"). Thus, the integral of the shaded area shown in Figure 1 between those two functions may correlate to the risk of radiation-induced leukemias, although the scale of the ordinate for the stem/progenitor cell survival curve described here may be arbitrary. Namely, the shaded shared area between the area beneath the stem/progenitor cell survival curve and the upper area of the lower curve, i.e., the minimum number of mutated stem/progenitor cells for the development of one case of leukemia as a function of radiation dose, may be the risk factor for radiation-induced leukemogenesis. Furthermore, when one incorporates corresponding data from p53-knockout mice (Fig. 1B) and other data from genetically modified animals, any modifications of shared areas suggest a decrease and/or an increase in risk of the incidence of experimental leukemogenesis. Such statistical relevance between the number of hemopoietic stem/progenitor cells and the induction of experimental leukemias can be applied also to the study of the incidence of benzene-induced leukemias. In the case of benzene-induced leukemias, the relevance of stem cell kinetics to the incidence of experimental leukemias is a function of changes in hemopoietic progenitor cells. In this article, such relevancies between the number and quality of stem/progenitor cells and the incidence of leukemias after radiation and/or benzene exposure with respect to biological modification after caloric restriction and/or modification of the state of oxidative stress are introduced after a brief description of the characteristics of hemopoietic progenitor cell function.

Materials and methods

Mice

C3H/He and C57BL/6 strain, male and female, with or without genetic modification for p53 deficiency [4] or thioredoxin overexpression [5] were used in the hemopoietic stem/progenitor cell research, radiation- or benzene-induced leukemogenesis followed by histopathological examination. Experimental animal protocols used were reviewed by the externally established peer-review panel, and maintained in the board-approved laboratory animal facility of the National Institute of Health Sciences of Japan.

Radiation and bone marrow transplantation

For a lethal dose of radiation (9.45 Gy) for bone marrow transplantation and a graded increased dose up to 5.0 Gy of x-ray irradiation for induction of hematopoietic malignancies, mice were subjected to a 200-kV/20 A pulse through a therapeutic x-ray irradiator (Shimadzu, Tokyo) with 1.0-mm aluminum and 0.6-mm copper filters, at a dose rate of 0.614 Gy/minute and a 56-cm focus surface distance. Whole-body irradiation (8.5 Gy) by gamma-ray

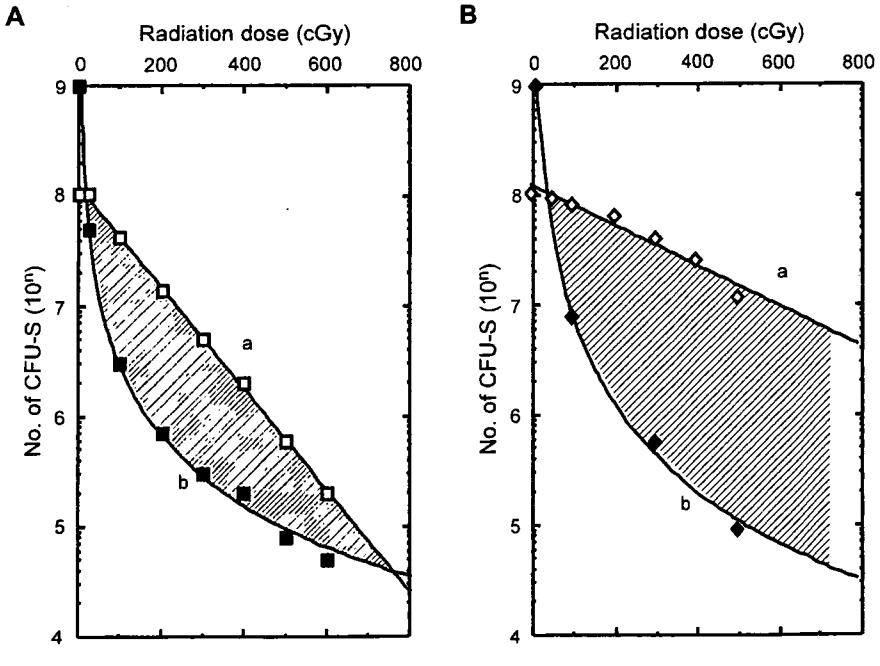

Figure 1. Possible risk of radiation-induced leukemia in wild-type mice (**A**) and p53-homozygous knockout mice (**B**). (**a**) Survival of stem cells after irradiation. (**b**) Minimum number of stem cells for development of a case of leukemia.

(^{137}Cs, at a dose rate of 0.101 Gy/minute, Gammacell 40 Exactor; MDS Nordion, Ottawa, Canada) with a 0.5-mm aluminum-copper filter was also given in the assay of colony-forming unit in spleen.

Benzene and benzene exposure

Benzene (CAS no. 71-43-2, MW 78.11) was purchased from Wako Fine Chemical Company (Osaka, Japan). Mice were randomly assigned to groups and individually housed. They were exposed to benzene in 1.3 m^3 inhalation chambers as described previously [6,7]. The benzene-exposed mice were exposed to 300 ppm of benzene 6 hours per day, 5 days per week for 2 weeks for short-term examination, and 26 weeks for leukemogenicity bioassay. The mice were supplied water ad libitum, but food pellets were withdrawn during the exposure.

Caloric restriction

For caloric restriction studies, a 77 kcal/week was maintained. Groups subjected to different caloric restriction timings were compared with groups not subjected to caloric restriction during lifetime for incidences of neoplasms followed by histopathological examination [8,9].

Assays for CFU-S and CFU-GM

For assay of hematopoietic colonization, colony-forming unit in spleen (CFU-S) [10] and colony-forming unit granulocyte macrophages (CFU-GM) [7,11] were evaluated. For CFU-GM assay, a semisolid methylcellulose culture, supplemented with 10 ng/mL murine granulocyte macrophage colony-stimulating factor (R&D Systems, Inc., Minneapolis, MN, USA) was conducted.

BUUV method

Hematopoietic progenitor cell-specific kinetic studies were evaluated by continuous labeling of bromodeoxyuridine for cycling cells, followed by UV exposure and hemopoietic colonization (BUUV method, details in [11,12]).

Gompertzean expression

Experimental survival curves were applied to Gompertz's law of mortality to examine lifespans and mortality rates in mice with ionizing radiation- and benzene-induced leukemias. (Detailed procedure of mathematical analysis by Gompertz-Makeham law of mortality is found in ref. [1].).

Results and discussion

Hemopoietic stem/progenitor cells as a target of experimental leukemogenesis

Because the major histopathological type of radiation-induced leukemia in p53-deficient mice was stem cell leukemia with trace evidence of myeloid differentiation, the possible target cells in leukemogenesis were supposed to be hemopoietic stem/progenitor cells [13]. Interestingly, p53-heterozygous deficiency also produced stem cell leukemia with loss of heterozygousity after graded increased doses of radiation exposure (unpublished observation). Therefore, to understand the mechanism underlying leukemogenesis induced by radiation and/or benzene exposure, current series of evidence regarding stem/progenitor cell characteristics are particularly important. Furthermore, in addition to the generation-age structure of hierarchic stem/progenitor cells, current knowledge on genes regulating kinetics in stem/progenitor cells (i.e., genes maintaining the long-term repopulating cells), genes in splenic colony-forming units, and genes in in vitro colony-forming units, is found to be particularly important for understanding development of leukemias. Because of the possible participation of negative regulators of stem/progenitor cell differentiation and self-renewal, such as *Notch* [14], *Wnt* [15], and *Sonic hedgehog* [16] signals, and *Bmi-1* [17] expression, a dormant fraction, about 80% in the hemopoietic stem/progenitor cell compartment, which does not incorporate bromodeoxyuridine (BrdUrd), is continuously maintained for lifetime after the development of this dormant fraction during the neonatal stage. The cycling fraction, on the other hand, incorporates BrdUrd continuously and about 20% of the total progenitor cell compartment is maintained throughout the lifespan. Furthermore, the doubling time of each progenitor cell compartment in the stem/progenitor hierarchy is facilitated in the order from immature progenitor cells with faster generation time to mature progenitor cells with slower generation time (data not shown). The size of dormant fractions slightly decreases with the age structure of progenitor cells. We previously observed that hemopoietic progenitor cells also maintain their immaturity with transforming growth factor-β (TGF-β) [18], as well as gap junctional intercellular communication, specifically with connexin-32, which was supposed to maintain the size of the immature stem/progenitor cell compartment, steady-state growth, regenerating potential after experimental chemical abrasion, and possibly function as a tumor suppressor for leukemogenesis.

Novel tool to evaluate hemopoietic progenitor-specific cell kinetics (BUUV method[1]) as a key parameter for leukemogenesis

The concept of a stem/progenitor cell pool and the daily outflow (i.e., production) of committed cells to erythropoietic, granulopoietic, and megakaryocytic lineages were also intensively studied by Cronkite and his associates from the 1960s to the 1970s. They determined the number of stem/progenitor cells undergoing DNA synthesis using tritiated thymidine (^{3}H-TdR) with a low specific radioactivity as well as the incorporation of ^{3}H-TdR with a cytocidal dose of high-specific activity for evaluating the cycling fraction [19]. In the early 1980s, Cronkite applied his knowledge on steady-state hematopoiesis to toxicological studies, not only to the radiation-induced, but also benzene-induced, hemopoietic toxicities and their consequence, namely,

[1]Continuous infusion of bromodeoxyuridine by osmotic minipump to label cycling cells in general is carried out, followed by UV exposure to kill labeled cells, and then allowing surviving stem cells to form hemopoietic colonies.

leukemogenesis [20]. Cell kinetic studies using ^{3}H-TdR with low- and high-specific activities provided a new paradigm of benzene- and other chemical-related hematotoxicities.

There are two technical limitations of the experimental and hematological use of ^{3}H-TdR. First, ^{3}H-TdR with a low-specific activity enables labeling of cycling cells, but not killing them, second, ^{3}H-TdR with a high-specific activity, enables the labeling and killing of cycling cells, but not the studying of long-term cell kinetics. The BUUV method established by Hirabayashi and coworkers [11,12] entails the purging of cells labeled by BrdUrd using UV-A light for evaluating the kinetics of hemopoietic progenitor cells, followed by colonization and other hematological evaluations (Fig. 2). The method enables long-term labeling of cycling cells for up to nearly a lifetime and the assay of the size of the cytocide fraction at anytime by exposure to UV-A light followed by relevant colonization assay methods and/or cell sorting. Although many similar methods were reported previously, none of them are appropriate for hemopoietic stem cell research. The reasons are as follows: In previous methods, UV-B and UV-C lights were used, not UV-A light, which resulted in serious errors. In the case of Pietrzyk et al. [21], they used highly toxic UV-C light, which that made progenitor cells mortal regardless of the labeling, and thus, made a real dormant fraction missing. In the case of Hagan and colleagues [22,23], they used UV-B light, and found plateau phases of a surviving colony fraction with increasing dose of UV-B fluence (J/m^2) after increasing the period of BrdUrd infusion. The fraction containing cycling one measured on the basis of colony formation still exponentially increases >90%. Use of UV-A and incorporation of BrdUrd in drinking water for long-term administration collaboratively provided a revolutionary paradigm for increasing the knowledge of kinetics in the hemopoietic stem/progenitor cell compartment.

A new discovery is the existence of a long-term and stable, dormant fraction. This is similar to crypt stem cells at the bottom of intestinal villi, described by Potten et al. [24], but never clearly observed in the hemopoietic system. The dormant fraction develops presumably after the early developmental stage of the neonatal period, which forms an orderly generation-age structure from a primitive CFU-S-13, mature CFU-S-9, and to an in vitro CFU-GM (21.7% ± 4.7%, 33.4% ± 3.3%, and 35.0% ± 3.7%, respectively [11]). Second, by BUUV assay, some disadvantages of in vitro labeling with ^{3}H-TdR and also with BrdUrd were consequently discovered; e.g., in vitro labeling artificially results in a marked overestimation of the percentage of the labeled fraction from 9.9% ± 4.8% to 37.4% ± 4.5%. The cycling fraction of CFU-GM is often labeled and assayed in vitro. The in vivo labeling assay value is

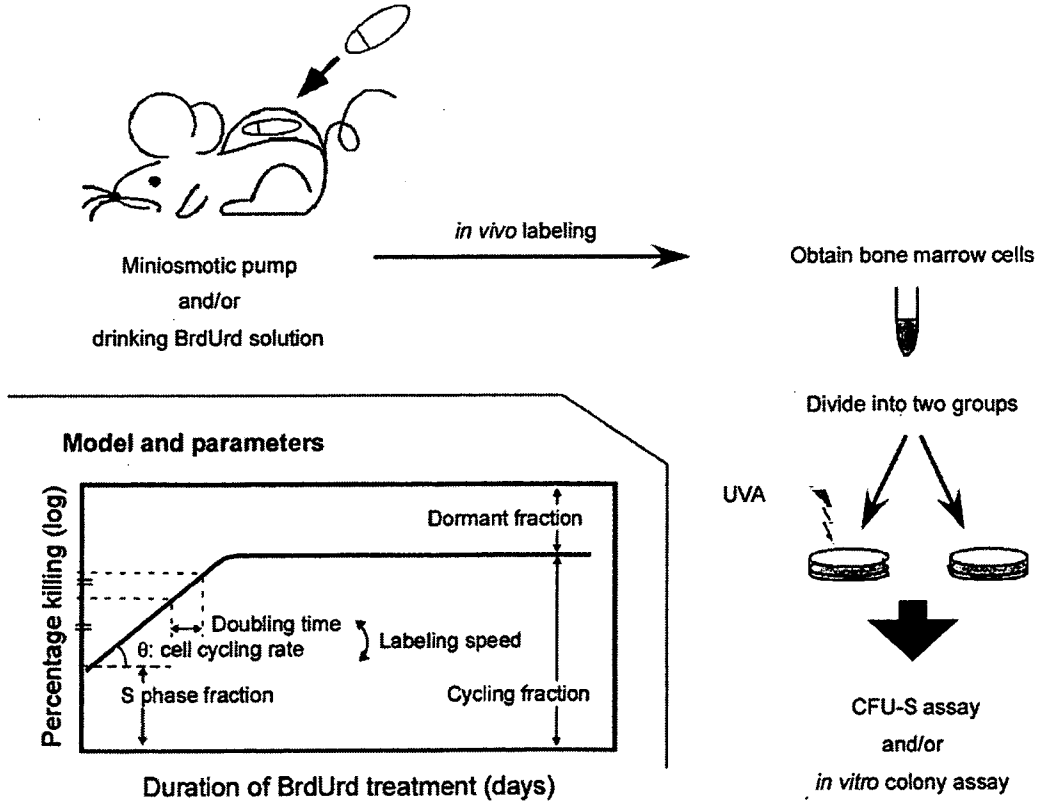

Figure 2. Bromodeoxyuridine UV method as a tool for evaluating size and other parameters of cycling stem cell fraction in vivo [12].

only slightly higher than the actual CFU-S cycling fraction when assayed by in vivo labeling, regardless of the labeling method; that is, intravenous injection or via drinking water (9.9% ± 4.8% vs 6.8% ± 4.8%; CFU-GM vs CFU-S-9, respectively). Many previous studies showed that CFU-GM and other in vitro colonies labeled with ^{3}H-TdR cytocide were nearly 60% in cycling, which was used as an indicator of the maturity of progenitor cells in vitro in terms of generation age, but are now considered artifacts.

The doubling time and the generation time of each progenitor cell compartment are also dependent on the age-structure, and the doubling times are from 35.2 hours in CFU-S-13, 48.5 hours in CFU-S-9 to 56.0 hours in CFU-GM, respectively [11]. For example, in the cases of caloric restriction and 3′-azido-3′-deoxythymidine treatment, both markedly decreased the cycling fraction of the hemopoietic stem/progenitor cell compartment [8,9,25].

Radiation-induced leukemogenesis and its prevention by caloric restriction

As shown in Figure 1A, the incidence of radiation-induced leukemias depends on two functions: one is stem/progenitor cell survival with graded increases in radiation dose and the other is the minimum number of potentially mutated stem/progenitor cells for the development of one case of leukemia vs graded increases in doses of radiation. Because the integral of the shaded channel area in Figure 1 decreases with the increase in radiation doses and the channel is closed at 6 to 7 Gy, radiation-induced leukemias are not supposed to develop at more than 6 to 7 Gy in the murine system. In the case of p53-deficient mice, however, despite radiation-induced damage, the survival of hemopoietic progenitor cells with the increase in radiation dose shows a much shallower survival curve (Fig. 1B, line "a"), owing to their escape from p53-dependent apoptosis; these cells may retain unrepairable DNA damage (data not shown; [13,26]). This modification of the survival curve of hemopoietic stem/progenitor cells deficient in p53 further increases the incidence of radiation-induced leukemias, and the incidence of leukemias following 5-Gy exposure keeps increasing up to 100% (unpublished data).

Next, we modified radiation-induced leukemogenesis by caloric restriction, because caloric restriction is the only nutritional factor that extends lifespan of experimental animals [27], and is supposed to attenuate radiation-induced leukemias [9]. The C3H/He mouse strain shows a high incidence of myeloid leukemias, with a low spontaneous incidence (of myeloid leukemia). Nonirradiated mice showed a 1% incidence of spontaneous myeloid leukemias with a median lifetime of 839 days. The incidence of myeloid leukemias increased up to 22.2% with a decrease in median lifetime to 697 days after the 3-Gy whole-body x-ray irradiation of mice. Various methods of caloric restriction induced a prominent decrease in the incidence of myeloid leukemias at 3 Gy; i.e., 9.5% in the group with caloric restriction for the rest of their lifetime immediately after the irradiation; 8.0% in the group with caloric restriction throughout their lifetime. No leukemia developed in groups not exposed to radiation (data not shown; [9]).

Along with the decrease in the incidence of myeloid leukemia in the group with caloric restriction, interestingly, the percentages of tumor-free mice consequently increased from 7.4% to 17.5% and 20.0%, in the group with caloric restriction for the rest of their lifetime after 3-Gy irradiation and in the group with caloric restriction throughout their lifetime, respectively. Nonirradiated group with caloric restriction also showed a statistically significant increase 10.1% to 46.4% in the percentage of tumor-free mice as compared with groups without caloric restriction.

Because caloric restriction decreased the number of hemopoietic stem/progenitor cells and the cycling fraction of hemopoietic progenitor cells, as evaluated by the BUUV method in these series of experiments, we conclude that caloric restriction decreases the incidence of radiation-induced leukemias via two mechanisms. First, the suppression of direct genotoxic leukemogenesis during the initiation stage, i.e., caloric restriction started before irradiation and continued until irradiation. Second, the suppression of indirect epigenetic leukemogenesis during the promotor stage, i.e., restriction started after irradiation and continued for lifetime. In these studies of caloric restriction, particular attention was focused on the number and cell cycle of hemopoietic stem/progenitor cells regardless of other suppressive factors that may also contribute to general oncogenesis, such as oncogene expression, DNA methylation, free radical formation, apoptosis induction and immunity activation, among others.

Benzene-induced hemopoietic toxicities and induction of leukemias, and their attenuation by thioredoxin overexpression

Cronkite was the first scientist who clearly recognized the relevance of the number and position of hemopoietic stem/progenitor cells in their kinetics with respect to the development of leukemias [28]. Consequently, his benzene exposure protocol successfully induced the first experimental benzene-induced leukemias; namely, the induction of a modest decrease in the number of hemopoietic progenitor cells that does not lead to extinction of such cells [2], which was after the first report of leukemogenicity induced in humans nearly 80 years ago [29]. He was interested in, and focused on, peculiar oscillatory changes in the numbers of bone marrow cells and hemopoietic progenitor cells, although laborious ^{3}H-TdR labeling for the complicated cell-cycle perturbation induced by benzene exposure could not help his group clarify the mechanism underlying cell-cycle oscillation. As reported by our group previously in *Experimental Hematology* [7], benzene exposure was found to be not only in mature blood cells, but also in hemopoietic stem/progenitor cells, a strong cell-cycle suppressor, due to clastogenic

damages suggested by an upregulation of topoisomerase III in the bone marrow [30]; however, cessation of benzene exposure during weekends induced rapid recovery of the cycling of the hemopoietic stem/progenitor cell fraction, which induced the repeated counter-oscillatory changes during the exposure period and resulted in a high frequency of epigenetic induction of hemopoietic malignancies (Fig. 3). Benzene and its major metabolites are negative in Ames-revertant mutagenesis assay, and induce a lesser amount of DNA adducts, which cannot explain in detail the mechanism underlying leukemogenicity. Benzene-induced cell-cycle perturbation observed in the present study may collaboratively cause clastogenic chromosomal damage induced by benzene mono-oxide and oxidative stress [30,31].

Conclusion from the base of bioinformatics: Experimental leukemogenesis and its attenuation with respect to related changes in Gompertzean survival curve

In the theoretical model of the mortality rate of human beings, studied by Gompertz [1] more than 180 years ago, he found that death rate during a unit time interval increases exponentially with lifetime. The Gompertzean expression can be applied to major mammalian species (Fig. 4A) [32]. The implication of Gompertzean linearity in experimental groups and changes in the slope linearity are considered to be based on an observation that lifespan may involve a function based on the multiplication of various life-threatening factors. Namely, the linearity is based on a system in which each lifespan-linked disease is independent and links to other diseases multiply (Eq. 1).

$$N'(t) = -rN(t)log(N(t)/K) \quad (1)$$

where $N(t)$ is number of individuals at time t, r is intrinsic growth rate, and K is number of individuals in equilibrium.

Furthermore, any continuous life-threatening factors except deaths from traffic accident, war, or epidemic infections, make Gompertzean linearity steeper (Fig. 4B: standard, "Std", to "Tox"). For example, in the case of mice exposed to graded increases in radiation dose, their lifespan shows continuously steeper curves from high-dose to zero-dose group, i.e., a steeper curve to a shallower

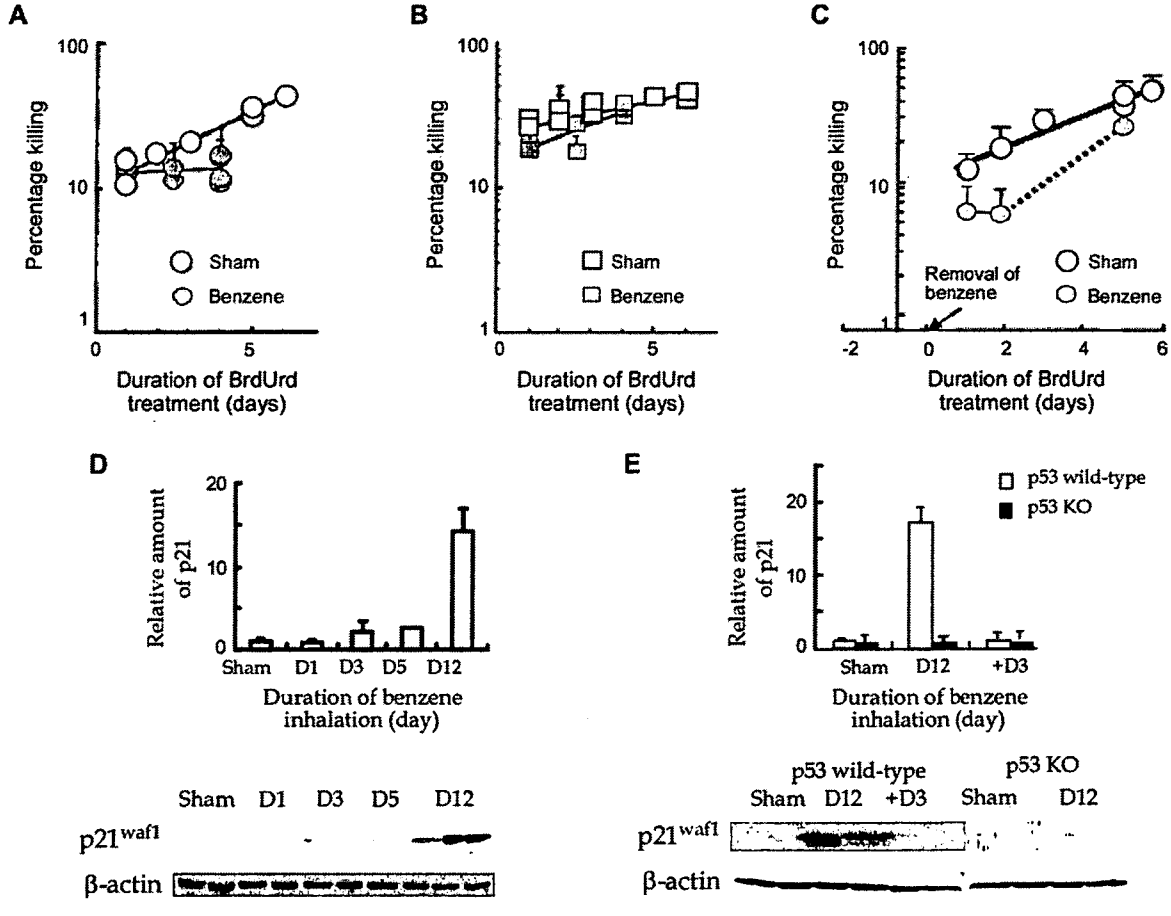

Figure 3. Benzene-induced cell-cycle arrest via p53-p21^{waf1} signal pathway [7]. (**A**) In wild-type mice, cell kinetics is stopping during the benzene inhalation (closed circles) vs sham control (open circles). (**B**) In p53-homozygous knockout mice, cell kinetics is maintained during benzene inhalation (closed squares) vs sham control (open squares). (**C**) After stopping benzene exposure, cell kinetics rapidly recovers in wild-type mice. (**D**) In wild-type mice, p21^{waf1} is upregulated during benzene inhalation. (**E**) In p53-homozygous knockout mice, p21^{waf1} is not changed during benzene inhalation. After stopping benzene inhalation, in wild-type mice, p21^{waf1} is downregulated immediately.

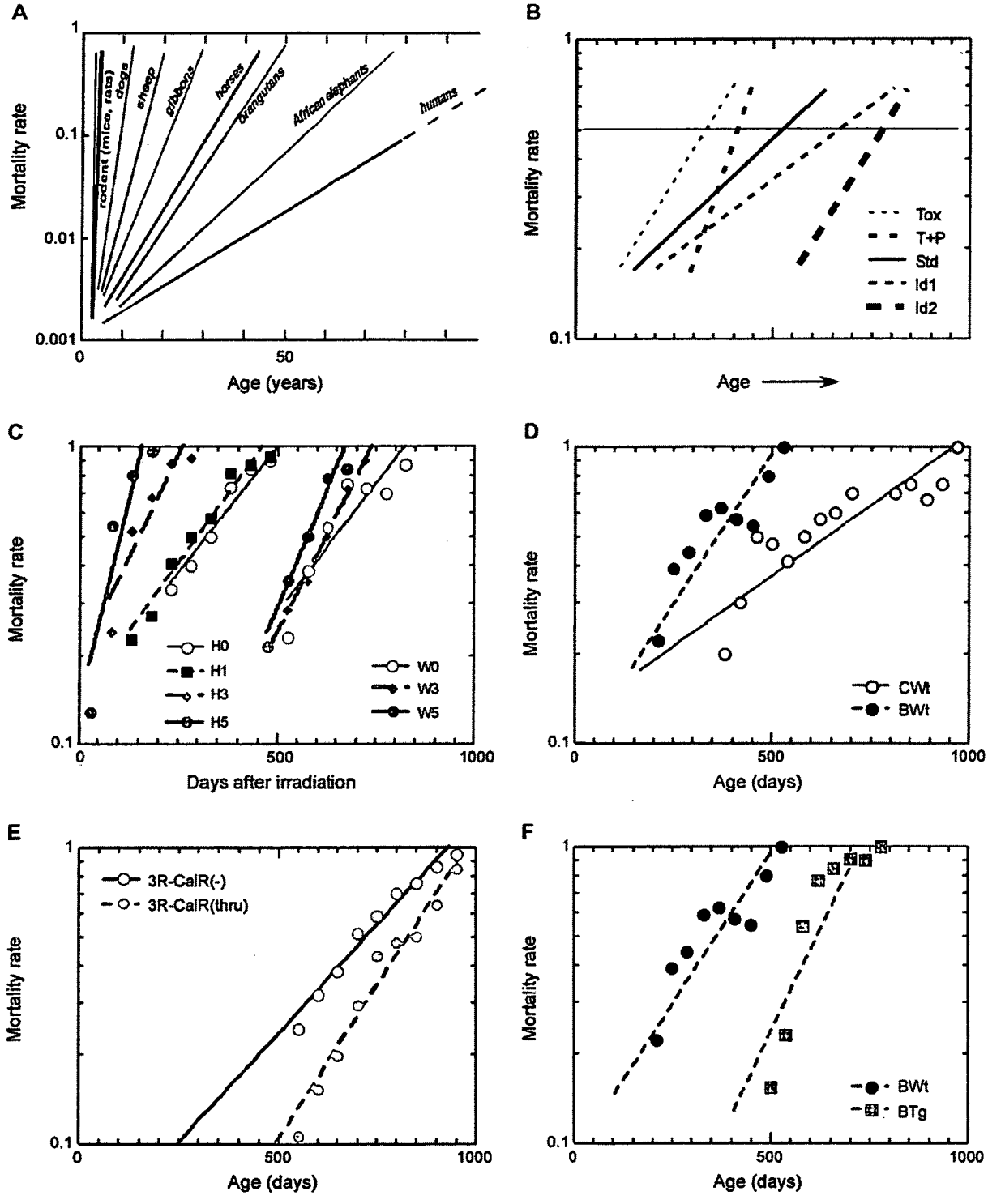

Figure 4. Gompertz's low of mortality was applied to examine lifespans and mortality rates in mice with ionizing radiation (IR)- and benzene-induced leukemias. (**A**) Lifespan in the steady-state animals, based on the life expectancy. (**B**) Gompertz model for lifespan in toxic changes and its attenuations. Tox = toxic state; T+P = toxic state with prevention; Std = standard; Id = ideal state). (**C,E**) Radiation-induced shortening of lifespan. (**C**) H0 to H5 = p53-heterozygous knockout mice with 0 to 5 Gy whole-body irradiation; W0 to W5 = wild-type mice with 0 to 5 Gy whole-body irradiation and its recovery by caloric restriction. (**E**) 3R-CalR(−); 3-Gy irradiation without caloric restriction, 3R-CalR(thru); 3-Gy irradiation with caloric restriction). Average caloric intake calculated was 77 kcal per week per mouse (i.e., 81.1% of the nonrestrict control). Detailed technical information for caloric restriction can be found elsewhere [9]. (**D,F**) Benzene-induced shortening of lifespan. (**D**) CWt = wild-type mice for sham control; BWt = wild-type mice with benzene exposure) and recovery by Trx overexpression. (**F**) BWt = wild-type mice with benzene exposure; BTg = thioredoxin overexpression mice with benzene exposure. Benzene was exposed at 300 ppm, 6 hours per day, 5 days a week, for 26 weeks. For Trx overexpression mice, detailed technical information can be found elsewhere [5,31].

curve (Fig. 4C). In Figure 4C, H0 through H5 indicate p53 heterozygous-deficient mice exposed to graded increases in dose of radiation (0–5 Gy), which show more steeper and shortened lifespans. Similarly, benzene-induced leukemias make the lifespan curve in the Gompertzean expression also steeper with benzene exposure (Fig. 4D). Although these slopes seem to be based on the incidence of various types of tumorigenesis, the slopes may be modified by other chronic factors, such as nutrition related to cardio- and/or renal-vascular diseases. Two prevention studies provide interesting prevention curves in Gompertzean expression; one on caloric restriction in radiation-induced leukemogenesis [9] and the other on thioredoxin overexpression against benzene toxicity [31], which shows potentially equivalent antioxidative functions (Fig. 4E and F). Gompertzean expression curves for toxic compounds and for inhibitory compounds shown in Figure 4C to F imply that the slopes for Gompertzean expression may be based on the model shown in Figure 4B (Fig. 4E corresponds to "T+P (Tox & Prevention)" in Fig. 4B; Fig. 4F corresponds to ideal prevention, "Id 2" in Fig. 4B.). The significance of differences in slopes in Gompertzean expression among the non-treated animals, animals treated with toxic compounds, and animals treated with inhibitory compounds, and possible deterministic factors for genomic stabilization, cell-cycle regulators and active caloric metabolic enzymes, among others, are not clearly understood. However, this relevance would be an important factor for elucidating the mechanism underlying toxicities vs prevention of lifespan.

Acknowledgments

The authors would like to thank the collaborators for valuable assistance. This work was supported in part by the fund from Nuclear Research of MEXT, Japan, the Human Sciences of Japan (KH31034, KHC1204), Grants-in-Aid (Nos.13670236, 15510064, 16590329 and 18510066) for Scientific Research C from the Japan Society for the Promotion of Sciences, and Risk Analysis Research on Food and Pharmaceuticals for Health and Labor Science Research Grants (H15-Chemicals-002, H16-Chemicals-002).

References

1. Gompertz B. On the nature of the function expressive of the law of human mortality, and on a new mode of determining the value of life contingencies. Pholos Trans Royal Soc (Lond). 1825;115:513–585.
2. Cronkite EP, Inoue T, Carsten AL, Miller ME, Bullis JE, Drew RT. Effects of benzene inhalation on murine pluripotent stem cells. J Toxicol Environ Health. 1982;9:411–421.
3. Cronkite EP. Hemopoietic stem cells: an analytic review of hemopoiesis. Pathobiol Annu. 1975;5:35–69.
4. Tsukada T, Tomooka Y, Takai S, et al. Enhanced proliferative potential in culture of cells from p53-deficient mice. Oncogene. 1993;8:3313–3322.
5. Mitsui A, Hirakawa T, Yodoi J. Reactive oxygen-reducing and protein-refolding activities of adult T cell leukemia-derived factor/human thioredoxin. Biochem Biophys Res Commun. 1992;186:1220–1226.
6. Cronkite EP, Bullis J, Inoue T, Drew RT. Benzene inhalation produces leukemia in mice. Toxicol Appl Pharmacol. 1984;75:358–361.
7. Yoon BI, Hirabayashi Y, Kawasaki Y, et al. Mechanism of action of benzene toxicity: cell cycle suppression in hemopoietic progenitor cells (CFU-GM). Exp Hematol. 2001;29:278–285.
8. Yoshida K, Inoue T, Hirabayashi Y, Matsumura T, Nemoto K, Sado T. Radiation-induced myeloid leukemia in mice under calorie restriction. Leukemia. 1997;11(suppl 3):410–412.
9. Yoshida K, Hirabayashi Y, Watanabe F, Sado T, Inoue T. Caloric restriction prevents radiation-induced myeloid leukemia in C3H/HeMs mice and inversely increases incidence of tumor-free death: implications in changes in number of hemopoietic progenitor cells. Exp Hematol. 2006;34:274–283.
10. Till JE, McCulloch EA. A direct measurement of the radiation sensitivity of normal mouse bone marrow cells. Radiat Res. 1961;14:213–222.
11. Hirabayashi Y, Matsuda M, Aizawa S, Kodama Y, Kanno J, Inoue T. Serial transplantation of p53-deficient hemopoietic progenitor cells to assess their infinite growth potential. Exp Biol Med (Maywood). 2002;227:474–479.
12. Hirabayashi Y, Matsumura T, Matsuda M, et al. Cell kinetics of hemopoietic colony-forming units in spleen (CFU-S) in young and old mice. Mech Ageing Dev. 1998;101:221–231.
13. Yoshida K, Aizawa S, Watanabe K, Hirabayashi Y, Inoue T. Stem-cell leukemia: p53 deficiency mediated suppression of leukemic differentiation in C3H/He myeloid leukemia. Leuk Res. 2002;26:1085–1092.
14. Milner LA, Kopan R, Martin DI, Bernstein ID. A human homologue of the Drosophila developmental gene, Notch, is expressed in CD34+ hematopoietic precursors. Blood. 1994;83:2057–2062.
15. Reya T, Duncan AW, Ailles L, et al. A role for Wnt signalling in self-renewal of haematopoietic stem cells. Nature. 2003;423:409–414.
16. Bhardwaj G, Murdoch B, Wu D, et al. Sonic hedgehog induces the proliferation of primitive human hematopoietic cells via BMP regulation. Nat Immunol. 2001;2:172–180.
17. Lessard J, Sauvageau G. Bmi-1 determines the proliferative capacity of normal and leukaemic stem cells. Nature. 2003;423:255–260.
18. Sasaki H, Matsuda M, Lu Y, et al. A fraction unresponsive to growth inhibition by TGF-beta among the high-proliferative potential progenitor cells in bone marrow of p53-deficient mice. Leukemia. 1997;11:239–244.
19. Cronkite EP. Kinetics of leukemic cell proliferation. Semin Hematol. 1967;4:415–421.
20. Cronkite EP. Regulation and structure of hemopoiesis: Its application in toxicology. In: Iron RD, ed. Toxicology of the Blood and Bone Marrow. New York: Raven Press; 1985. p. 17–38.
21. Pietrzyk ME, Priestley GV, Wolf NS. Normal cycling patterns of hematopoietic stem cell subpopulations: an assay using long-term in vivo BrdU infusion. Blood. 1985;66:1460–1462.
22. Hagan M, Patchen M, Weinberg S, MacVittie T. Erythroid progenitor (BFU-E, CFU-E) proliferation as inferred from 5′bromodeoxyuridine labeling. Exp Hematol. 1994;22:1221–1226.
23. Hagan MP, MacVittie TJ. CFUs kinetics observed in vivo by bromodeoxyuridine and near-UV light treatment. Exp Hematol. 1981;9:123–128.
24. Potten CS, Chadwick C, Ijiri K, Tsubouchi S, Hanson WR. The recruitability and cell-cycle state of intestinal stem cells. Int J Cell Cloning. 1984;2:126–140.
25. Inoue T, Cronkite EP, Hirabayashi Y, Bullis JE Jr, Mitsui H, Umemura T. Lifetime treatment of mice with azidothymidine (AZT) produces myelodysplasia. Leukemia. 1997;11(suppl 3):123–127.

26. Hirabayashi Y, Matsuda M, Matumura T, et al. The p53-deficient hemopoietic stem cells: their resistance to radiation-apoptosis, but lasted transiently. Leukemia. 1997;11(suppl 3):489–492.
27. MacCay CM, Crowell MF, Maynard MF. The effect of retarded growth upon the length of the lifespan and upon the ultimate body size. J Nutr. 1935;10:63–79.
28. Cronkite EP, Bullis J, Inoue T, Drew RT. Benzene inhalation produces leukemia in mice. Toxicol Appl Pharmacol. 1984;75:358–361.
29. Delore P, Borgomano C. Leucémie aiguë au cours de l'intoxication benzénique. Sur l'origine toxique de certaines leucémies aiguës et leurs relations avec less anémies graves. J de méd de Lyon. 1928;9:227–233.
30. Yoon BI, Li GX, Kitada K, et al. Mechanisms of benzene-induced hematotoxicity and leukemogenicity: cDNA microarray analyses using mouse bone marrow tissue. Environ Health Perspect. 2003;111: 1411–1420.
31. Li GX, Hirabayashi Y, Yoon BI, et al. Thioredoxin overexpression in mice, model of attenuation of oxidative stress, prevents benzene-induced hemato-lymphoid toxicity and thymic lymphoma. Exp Hematol. 2006;34:1687–1697.
32. Trosko JE, Inoue T. Oxidative stress, signal transduction, and intercellular communication in radiation carcinogenesis. Stem Cells. 1997; 15(suppl 2):59–67.

Oncogene (2007), 1–13

www.nature.com/onc

ORIGINAL ARTICLE

Epigenetic silencing of *prostaglandin E receptor 2 (PTGER2)* is associated with progression of neuroblastomas

Y Sugino[1,2,3], A Misawa[1,2], J Inoue[1,2], M Kitagawa[4], H Hosoi[3], T Sugimoto[3], I Imoto[1,2,5] and J Inazawa[1,2,5,6]

[1]*Department of Molecular Cytogenetics, Medical Research Institute and School of Biomedical Science, Tokyo Medical and Dental University, Tokyo, Japan;* [2]*Core Research for Evolutionary Science and Technology of the Japan Science and Technology Corporation, Saitama, Japan;* [3]*Department of Pediatrics, Kyoto Prefectural University of Medicine, Kyoto, Japan;* [4]*Department of Pathology and Immunology, Graduate School, Tokyo Medical and Dental University, Tokyo, Japan;* [5]*Department of Genome Medicine, Hard Tissue Genome research Center, Graduate School, Tokyo Medical and Dental University, Tokyo, Japan and* [6]*21st Century Center of Excellence Program for Molecular Destruction and Reconstitution of Tooth and Bone, Tokyo Medical and Dental University, Tokyo, Japan*

We previously identified a cluster of prostanoid receptor genes, *prostaglandin D2 receptor (PTGDR)* and *prostaglandin E receptor 2 (PTGER2)*, as possible targets for DNA methylation in advanced types of neuroblastoma (NB) using bacterial artificial chromosome array-based methylated CpG island amplification method. Among them, in this study, we found that *PTGER2* was frequently silenced in NB cell lines, especially in those with *MYCN* amplification, through epigenetic mechanisms. In NB cell lines, DNA methylation pattern within a part of CpG island was inversely correlated with *PTGER2* expression, and histone H3 and H4 deacetylation and histone H3 lysine 9 methylation within the putative promoter region were more directly correlated with silencing of this gene. Methylation of *PTGER2* was observed more frequently in advanced-type of primary NBs compared with early-stage tumors. Growth of NB cells lacking endogenous PTGER2 expression was inhibited by restoration of the gene product by transient and stable transfection. A PTGER2-selective agonist, butaprost, increased intracellular cyclic adenosine monophosphate (cAMP) level, inhibited cell growth and induced apoptosis of NB cells stably expressing exogenous PTGER2. 8-Bromo-cAMP also inhibited growth of NB cells lacking PTGER2 expression, but not cells expressing this gene. Taken together, it is suggested that NB cells may lose responsiveness to PTGER2-mediated growth inhibition/apoptosis through epigenetic silencing of PTGER2 and/or disruption of downstream cAMP-dependent pathway during the neuroblastomagenesis.
Oncogene advance online publication, 28 May 2007; doi:10.1038/sj.onc.1210550

Keywords: neuroblastoma; PTGER2; tumor suppressor; DNA methylation; histone modification; cAMP

Correspondence: Dr J Inazawa, Department of Molecular Cytogenetics, Medical Research Institute, Tokyo Medical and Dental University, 1-5-45 Yushima, Bunkyo-ku, Tokyo 113-8510, Japan.
E-mail: johinaz.cgen@mri.tmd.ac.jp
Received 20 February 2007; revised 23 March 2007; accepted 26 March 2007

Introduction

Neuroblastoma (NB) is one of the most common pediatric solid tumors of neural-crest origin. The outcome of this disease is highly heterogeneous: older patients frequently develop metastatic disease with extremely aggressive progression, whereas spontaneous regression is common in infants and in early-stage NB tumors (Westermann and Schwab, 2002; Brodeur, 2003). Although numerous genetic abnormalities, including the *MYCN* amplification, are involved in development and/or progression of NB, the molecular mechanisms responsible for the pathogenesis of aggressive NB remain unclear. Epigenetic alterations such as hypermethylation of promoter sequences, with consequent silencing of tumor-suppressor genes, such as *CASP8*, *RASSF1A*, *CD44* and *TSP-1* can play important roles in the pathogenesis of NB (Teitz *et al.*, 2000; Yan *et al.*, 2003; Yang *et al.*, 2003, 2004). Therefore, exploration of hypermethylated CpG-rich sequences in NB cell genomes could accelerate identification of unknown tumor suppressors whose loss contributes to progression of this disease.

Recently, we developed 'bacterial artificial chromosome (BAC) array-based methylated CpG-island amplification (MCA)' (BAMCA; Inazawa *et al.*, 2004), which incorporates our custom-made BAC-based genomic DNA array (Inazawa *et al.*, 2004) in combination with MCA (Toyota *et al.*, 1999), as a method for detecting aberrantly methylated sequences in the human genome. When we applied BAMCA to NB genomes using aggressive NB cell lines and stage 1 'nonaggressive' primary NB tumors as test and reference samples, respectively, followed by expression and methylation analyses of candidate targets, we successfully identified *NR1I2* as a novel tumor-suppressor candidate that is often silenced by DNA methylation in advanced type of this disease (Misawa *et al.*, 2005). In the process, we also identified several possible targets other than *NR1I2* for methylation-mediated silencing in advanced NB. Since identification of additional epigenetic abnormalities in

NB should lead not only to better understanding of the pathogenesis of this disease, but also to development of new diagnostic markers and/or therapeutic strategies (Abe *et al.*, 2005), determining the significance of each candidate tumor-suppressor gene inactivated by epigenetic mechanisms in NB will be highly valuable. Among possible targets, in the study reported here we analysed two genes, *prostaglandin E receptor 2* (*PTGER2*) and *prostaglandin D2 receptor* (*PTGDR*), both are located within the same BAC and encode receptors for subtypes of prostaglandin E2 (PGE2) and D2 respectively, and identified *PTGER2* as a candidate tumor suppressor for NB.

Results

Analysis of PTGDR *and* PTGER2 *expression in NB cell lines*
In our previous report (Misawa *et al.*, 2005), we described a strategy for identifying epigenetically silenced tumor-suppressor genes through exploration of aberrantly methylated sequences in the NB genome. During that program, *PTGDR* and *PTGER2*, within one BAC clone (RP11–262M8) at 14q22.1, were identified as possible targets for inactivation through DNA methylation (Figure 1a). To determine whether those genes might be silenced in NB, we examined expression of *PTGDR* and *PTGER2* mRNAs in a panel of 20 NB cell lines by reverse transcription (RT)–PCR. Expression of *PTGDR* was lost or decreased in most of the cell lines compared with normal adrenal gland and brain, whereas *PTGER2* expression was lost or decreased in eight lines and detected in 12 lines (Figure 1b). All eight lines that lacked expression of *PTGER2* showed amplification of *MYCN*, whereas only five of the 12 *PTGER2*-expressing lines did ($P=0.015$, Fisher's exact test).

Restoration of PTGDR *and* PTGER2 *expression by 5-aza-dCyd and TSA*
To investigate whether DNA demethylation could restore expression of *PTGDR* and *PTGER2* mRNAs in NB cells lacking them, we treated NB cells with 1 or 5 μM of 5-aza 2′-deoxycytidine (5-aza-dCyd), a methyltransferase inhibitor, for 5 days and/or 100 ng/ml of trichostatin A (TSA), a histone deacetylase inhibitor, for the last 12 h. Induction of *PTGDR* and *PTGER2* mRNAs occurred after treatment with 5-aza-dCyd in cells lacking expression of the genes (Figure 1c). Restoration of mRNA expression was also observed for both genes, especially *PTGER2*, after treatment with TSA alone. However, a greater elevation in expression was observed in cells treated with 5-aza-dCyd and TSA compared with those treated with 5-aza-dCyd alone, suggesting that DNA methylation and histone modification, including deacetylation of histones, may be cooperatively involved in silencing these two genes.

Methylation of PTGDR *and* PTGER2 *CpG islands in NB cell lines*
We examined the methylation status of CpG islands of the *PTGDR* and *PTGER2* genes predicted by the CpGPLOT program (http://www.ebi. ac.uk/emboss/cpgplot/, Figure 2a). Bisulfite-sequencing revealed aberrant DNA hypermethylation throughout the CpG island of *PTGDR* in four NB cell lines, regardless of expression levels (Figure 2b). On the other hand, aberrant DNA hypermethylation was observed within Region 3 and part of Region 2 of the *PTGER2* CpG island in three cell lines (IMR32, GOTO and SJ-N-CG) that lack expression of *PTGER2*, while this island was hypomethylated in SH-SY5Y expressing the gene. We performed combined bisulfite restriction analysis (COBRA) in a larger set of NB cell lines to confirm the relationship between expression and methylation status within the whole CpG island of *PTGDR* and within Region 3 or part of Region 3 (Region 3-A) of the *PTGER2* CpG island (Figure 2b and Supplementary Figure S1). Methylated alleles were predominant in most of the NB lines lacking *PTGER2* expression, and unmethylated alleles were always detected in cells that expressed this gene. For *PTGDR*, however, no clear relationship was observed between gene expression and methylation status of the CpG island. These results prompted us to characterize further the *PTGER2* gene as a candidate tumor suppressor inactivated through epigenetic mechanism.

Promoter activity of the CpG island of PTGER2
We performed reporter assays to determine whether the CpG island of *PTGER2*, whose methylation status was inversely correlated with gene expression, possessed promoter activity. Unexpectedly, fragment 3, where methylation was observed in NB cell lines lacking expression of *PTGER2*, revealed little promoter activity, whereas upstream fragment 1 showed remarkable activity (Figure 2c), suggesting that methylation within Region 3 of the *PTGER2* CpG island may not directly inhibit a promoter activity for gene expression, but indirectly contribute to silencing of *PTGER2* through additional epigenetic mechanisms.

Chromatin immunoprecipitation assay
Since the results of our promoter assays suggested that epigenetic mechanisms other than DNA methylation might directly regulate transcription of *PTGER2*, we postulated that histone acetylation and/or methylation might determine expression of *PTGER2* (Wolffe and Matzke, 1999; Schubeler *et al.*, 2000; Jones and Baylin, 2002; Kondo *et al.*, 2003; Nakagawachi *et al.*, 2003; Lorincz *et al.*, 2004; Stirzaker *et al.*, 2004; Strunnikova *et al.*, 2005; Azuara *et al.*, 2006; Frigola *et al.*, 2006; Yamada *et al.*, 2006), and examined status of histone modification by means of chromatin immunoprecipitation (ChIP) assays using primers designed within the putative promoter region (Figure 2a). Acetylated histone H3- and H4-binding fragments were decreased in gene-nonexpressing CHP134, SJ-N-CG and GOTO cell lines, as compared with gene-expressing SK-N-AS and SH-SY5Y cell lines

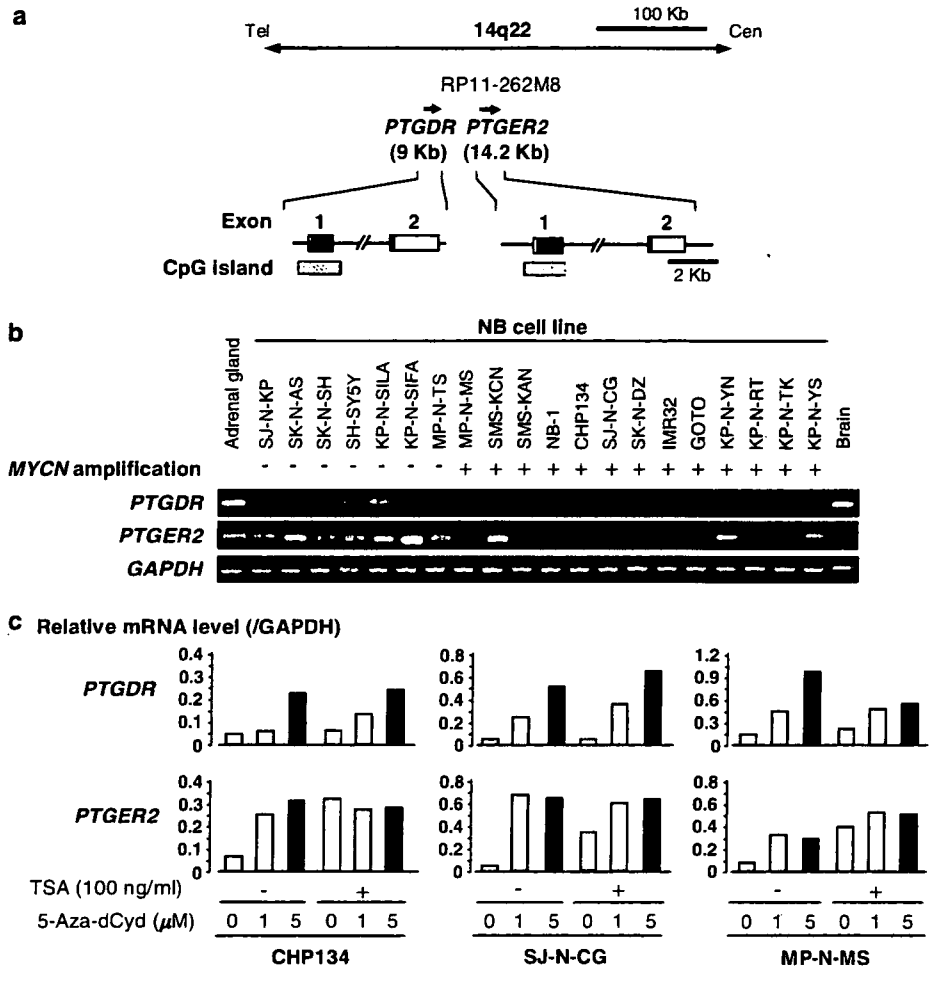

Figure 1 *PTGER2* and *PTGDR* are candidate targets for silencing in NB cells through DNA methylation. (**a**) Genomic structure of the *PTGDR* and *PTGER2* genes within the RP11–262M8 BAC clone, which was detected as one of BAC clones containing abnormally methylated sequences by BAMCA using two NB cell lines (GOTO and IMR32) as test samples and stage 1 NB tumors as control samples (Misawa *et al.*, 2005). Open and filled boxes represent untranslated and coding exonic sequences respectively; hatched boxes indicate 1479 and 1482 bp CpG islands that exist around exon 1 of each gene, respectively. (**b**) RT–PCR analysis of *PTGDR* and *PTGER2* mRNAs in normal adrenal gland, normal brain and NB cell lines with (+) or without (−) amplification of *MYCN* (Saito-Ohara *et al.*, 2003). Expression of *GAPDH* served as an internal control. (**c**) Representative results of RT–PCR analysis to reveal *PTGDR* and *PTGER2* mRNA expression in NB cell lines with (+) and without (−) treatment with 5-aza-dCyd and/or TSA, with *GAPDH* expression as an internal control. PCR products were electrophoresed in 3% agarose gel, and the band quantification was done with LAS-3000 (Fujifilm). Expression levels of *PTGDR* and *PTGER2* mRNA were normalized by that of *GAPDH* amplified at the same time. Experiments were repeated two times.

(Figure 2d). On the other hand, the di- and tri-methylated histone H3 lysine 9- (H3K9-) binding fragment was increased in the CHP134, SJ-N-CG and GOTO cell lines compared with SK-N-AS and SH-SY5Y cell lines (Figure 2d), suggesting that around the promoter region of *PTGER2*, histones H3 and H4 are hypoacetylated and histone H3K9 is di- and trimethylated in NB cells lacking expression of this gene and those status of histone modification may be associated with DNA methylation within Region 3 of the *PTGER2* CpG island. This observation is consistent with the restoration of *PTGER2* expression by TSA and the observed synergistic effect of TSA together with 5-aza-dCyd (Figure 1c).

Methylation and expression of PTGER2 *in primary NB tumors*

To determine whether aberrant methylation of *PTGER2* also takes place in primary NBs, we performed methylation analyses in a panel of surgical samples using bisulfite sequencing, COBRA and methylation-specific PCR (MSP). Several stage 4 tumors showed more or less aberrant methylation within Region 3 of the *PTGER2* CpG island (Figure 3a and Supplementary Figure S1), whereas the control normal adrenal gland or stage 1 and 4S tumors did not. Using primers designed within the Region 3 (Figure 3a) based on the localization pattern of methylation, we investigated the methylation status of the Region 3 within the *PTGER2*

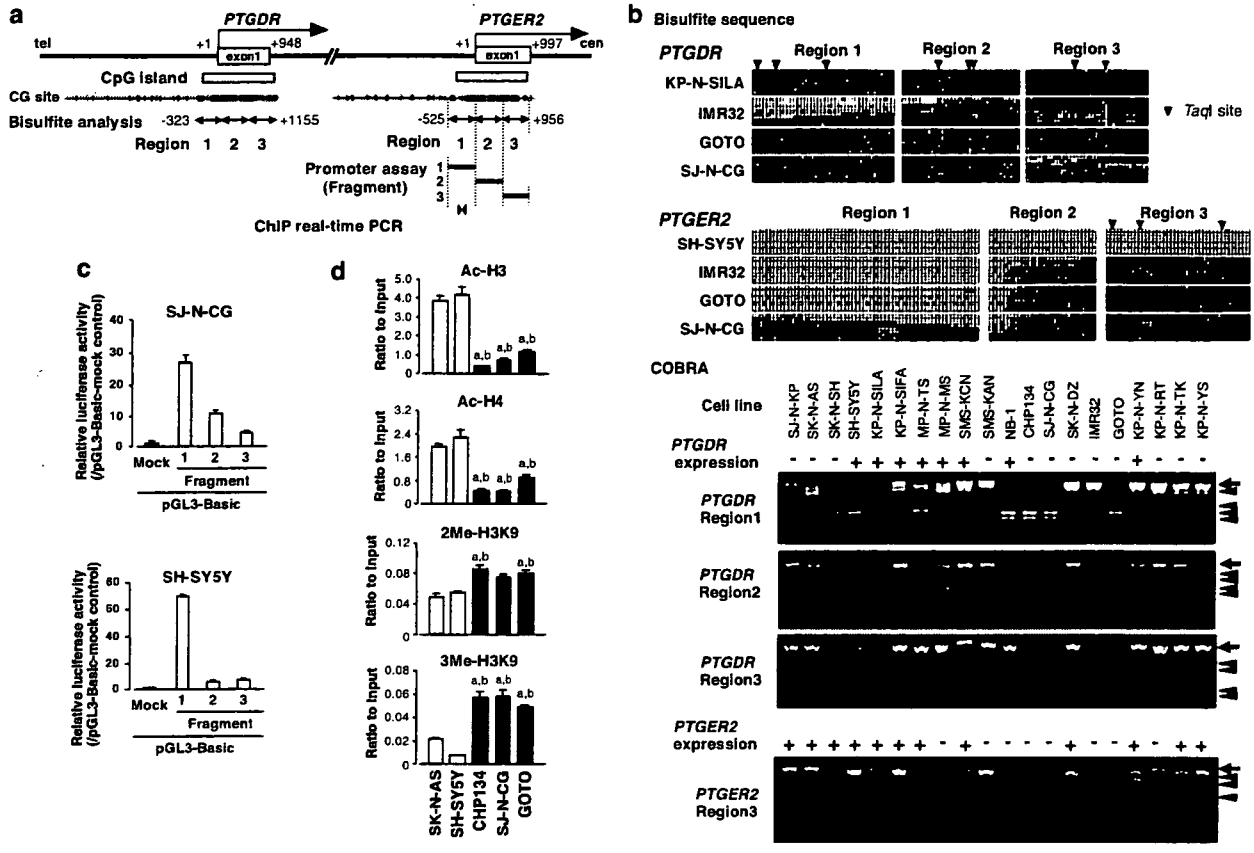

Figure 2 Association of DNA methylation and histone modification with expression status of *PTGER2*. (**a**) Map of the CpG islands (stippled bars) around the first exons of PTGDR and PTGER2. CpG sites are represented by vertical marks. Regions of each gene (Regions 1–3) examined for methylation by COBRA and bisulfite sequencing, are indicated by closed arrows. Fragments of *PTGRE2* examined in promoter assays (Fragments 1–3) are indicated by horizontal bars. The region analysed by ChIP-PCR is indicated below the map. (**b**) Left: Results of bisulfite sequencing of the CpG islands of *PTGDR* or *PTGER2* in *PTGDR* and *PTGER2* nonexpressing NB cell lines (IMR32, GOTO and SJ-N-CG) and expressing cell lines (KP-N-SILA or SH-SY5Y). Open and filled squares represent unmethylated and methylated CpG sites, respectively, and each row represents a single clone. *Taq*I restriction sites are indicated by black arrowheads. Right: Results of COBRA experiments involving Region 1–3 of the CpG island of *PTGDR* and Region 3 of the CpG island of *PTGER2* in NB cell lines with (+) or without (−) expression of each gene. PCR products were restricted by *Taq*I. Arrows indicate unmethylated alleles; arrowheads, methylated alleles. (**c**) Promoter activity of the *PTGER2* CpG island. pGL3 basic empty vectors (mock) and reporter constructs, each containing one of three different sequences within CpG island (Fragments 1–3 in Figure 2a), were transfected into a *PTGER2*-expressing cell line (SH-SY5Y) and a nonexpressing cell line (SJ-N-CG). Luciferase activities were normalized versus an internal control. The data presented are the means±s.d. of three separate experiments, each performed in triplicate. (**d**) ChIP-real time PCR assay quantitatively showing the status of histone acetylation and methylation of the *PTGER2* promoter region in NB cells *in vivo*. ChIP was performed using antibodies against acetylated histone H3 (Ac-H3), acetylated histone H4 (Ac-H4), dimethylated histone H3-lysine 9 (2Me-H3K9) and trimethylated histone H3-lysine 9 (3Me-H3K9). Experiments were performed using crosslinked extracts from PTGER2-expressing cell lines SK-N-AS and SH-SY5Y (open bars) and from PTGER2-nonexpressing cell lines CHP134, SJ-N-CG and GOTO (closed bars); immunoprecipitated samples containing the *PTGER2* promoter region were amplified by a quantitative real-time PCR (Figure 2b). A portion of the sonicated chromatin before immunoprecipitation (input) was served as a positive control for normalization, and the relative ratio to input was calculated. Differences among multiple comparisons were analysed by one-way ANOVA with subsequent Scheffé's tests: (**a**) versus SK-N-AS; (**b**) versus SH-SY5Y. All, $P<0.05$.

CpG island in all 49 surgically resected primary NBs and two ganglioneuromas. Methylation of Region 3 was detected in 12 of the 49 tumors (24.5%, Figure 3a), but not in ganglioneuromas. Of those 12 cases, four were in stage 1, 2, 3 and 4S tumors, whereas eight cases were in stage 4 ($P=0.0004$, Fisher's exact test; Figure 3b). The results of the MSP experiments were consistent with those from bisulfite sequencing (Figure 2b). Notably, eight of the nine tumors (88.9%) with *MYCN* amplification showed methylation, whereas only four of 40 tumors (10%) without amplification showed methylation ($P<0.0001$, Fisher's exact test; Figure 3b).

Expression levels of *PTGER2* mRNA in 39 primary NB tumors were evaluated by real-time quantitative RT–PCR. No significant difference was also observed between methylated and unmethylated NB cases as well as between *MYCN*-amplified and *MYCN*-unamplified NB cases ($P=0.6932$ and 0.7003, respectively, Student's *t*-test; Figure 3c). Since we conjectured that nontumorous cells such as leukocytes and endothelial cells might disturb accurate evaluation of expression levels of

PTGER2 in primary NBs, we performed immunohistochemical analysis using PTGER2-specific antibody to evaluate expression patterns in more detail. Matured ganglion cells in ganglioneuroma (Figure 3d) and NB cells differentiating to ganglion-like cells, seen mainly in stage 1 tumors with good prognosis (Figure 3e), were strongly stained with PTGER2, while the undifferentiated small round cells filling stage 4 tumors were stained weakly or not at all (Figures 3f and g). Endothelial cells and infiltrating cells, such as lymphocytes and macrophages, were also strongly stained (Figures 3f and g), suggesting that evaluation of *PTGER2* mRNA expression in whole NB samples might be affected by contamination with those normal tissue components.

Suppression of NB cell growth after restoration of PTGER2 *expression*

To gain further insight into the potential role of *PTGER2* loss in NB carcinogenesis, we investigated whether restoration of the gene product would suppress growth of NB cells lacking endogenous PTGER2. We used two kinds of PTGER2-expression constructs, a Myc-tagged full coding sequence of *PTGER2* (pcDNA-*PTGER2*-Myc) and one without epitope tag (pcDNA-*PTGER2*), with a mock construct (pcDNA-mock) as a control. Two (SJ-N-CG) or three (GOTO) weeks after transfection and subsequent selection of drug-resistant colonies, the number of large colonies produced by *PTGER2*-transfected SJ-N-CG and GOTO cells decreased markedly compared to cells containing empty vector, regardless of the existence of myc-epitope in the C-terminus (Figure 4a and Supplementary Figure S2). After transient transfection, typical apoptotic changes, such as condensation or fragmentation of nuclear chromatin, were observed more frequently in PTGER2-Myc-positive NB cells compared with either PTGER2-Myc-negative cells or control GFP-Myc-transfected cells (Figure 4b). Furthermore, stably *PTGER2*-transfected NB cells established from the SJ-N-CG and GOTO cell lines (Supplementary Figure S3a), showed a lower growth rate possibly in a PTGER2-expression level-dependent manner compared to cells transfected with control empty vector alone (mock, Figure 4c and Supplementary Figure S3b).

Effects of PGE2, butaprost and 8-Bromo-cAMP (8-Br-cAMP) on growth of NB cells

Since PTGER2 mediates a part of PGE2 signaling (Narumiya *et al.*, 1999), we examined whether PGE2 would affect growth of NB cells expressing PTGER2, using stable *PTGER2* transfectants of SN-J-CG and their control counterparts (empty-vector clones). Since transfectants established from GOTO cells were not resistant to culture with serum concentrations lowered to $\leqslant 1\%$ to reduce the effect of native PGE2 in serum, only SN-J-CG transfectants were available for the experiment. In mock transfectants, as in the DLD-1 colon-cancer cell line in which butaprost promoted cell growth (Castellone *et al.*, 2005), treatment with PGE2 for 72 h induced an increase in cell growth compared to treatment with vehicle alone (Figure 5a). In cells stably expressing PTGER2, on the other hand, almost no increase in cell growth was observed after treatment with PGE2 compared with vehicle alone, suggesting that growth of NB cells might be accelerated by signaling mediated through receptors for PGE2 other than PTGER2, but inhibited by signaling through PTGER2.

To confirm this hypothesis we examined growth of stable PTGER2 transfectants after treatment with a PTGER2-specific agonist, butaprost. The number of SJ-N-CG cells stably expressing PTGER2 was dramatically decreased after 72-h incubation with butaprost compared with vehicle alone, while the number of mock-transfected cells showed almost no change (Figure 5b), suggesting that signaling mediated by PTGER2, but not by other subtypes of PGE2 receptors, might specifically inhibit growth of NB cells. The same doses of butaprost promoted growth of the DLD-1 cell line. We performed fluorescence-activated cell sorting (FACS) analysis to analyse further the mechanism behind the antiproliferative effect of butaprost on NB cells. Butaprost treatment resulted in accumulation in the sub-G_1 phase of SJ-N-CG cells stably expressing PTGER2 (Figure 5c), suggesting that butaprost exerts its growth-inhibitory effect at least partly through induction of apoptosis mediated by PTGER2. Butaprost-induced apoptotic changes in SJ-N-CG cells stably expressing PTGER2 were also confirmed by terminal deoxynucleotidyl transferase (TdT)-mediated dUTP nick end-labeling (TUNEL) assay (Figure 5d). Under low-serum condition without butaprost treatment, stable PTGER2 transfectants resulted in an accumulation of cells in G_0–G_1 and a decrease in S and G_2/M phase cells compared with control counterparts (Figure 5c), suggesting that PTGER2 protein may arrest NB cells at the G_1-S checkpoint (G_0–G_1 arrest). However, no significant increase in the sub-G_1 phase was observed in stable PTGER2 transfectants compared with control counterparts (Figures 5c and d).

Since PTGER2 couples to G proteins and increases the intracellular concentration of cAMP (Narumiya *et al.*, 1999), we postulated that increased intracellular cAMP might play a role in inhibiting growth of NB cells. To test this hypothesis, we examined whether stimulation of PTGER2 would induce elevation of intracellular cAMP content in stable PTGER2 transfectants of the SJ-N-CG cell line. After treatment with butaprost, a distinct increase in cAMP was observed in these transfectants, whereas no increase in cAMP occurred in mock transfectants (Figure 5b). We further examined whether increasing intracellular cAMP using a cAMP analog, 8-Br-cAMP, would mimic the effect of butaprost on growth of NB cells. Growth of GOTO and SJ-N-CG cells, which lack expression of PTGER2, was inhibited by 8-Br-cAMP, whereas growth of SJ-N-KP and KP-N-SIFA, which express PTGER2, showed almost no change (Figure 6a). FACS analysis showed accumulation of GOTO and SJ-N-CG cells in the sub-G_1 phase after treatment with 8-Br-cAMP (Figure 6a).